Journal of Quantitative Spectroscopy & Radiative Transfer 142 (2014) 93–108

Contents lists available at ScienceDirect

Journal of Quantitative Spectroscopy & Radiative Transfer

journal homepage: www.elsevier.com/locate/jqsrt

IUPAC critical evaluation of the rotational–vibrational spectra of water vapor. Part IV. Energy levels and transition wavenumbers for $D_2{}^{16}O$, $D_2{}^{17}O$, and $D_2{}^{18}O$

Jonathan Tennyson [a,*], Peter F. Bernath [b], Linda R. Brown [c], Alain Campargue [d], Attila G. Császár [e], Ludovic Daumont [f], Robert R. Gamache [g], Joseph T. Hodges [h], Olga V. Naumenko [i], Oleg L. Polyansky [a,i], Laurence S. Rothman [j], Ann Carine Vandaele [k], Nikolai F. Zobov [l], Nóra Dénes [e], Alexander Z. Fazliev [i], Tibor Furtenbacher [e], Iouli E. Gordon [j], Shui-Ming Hu [m], Tamás Szidarovszky [e], Irina A. Vasilenko [i]

[a] Department of Physics and Astronomy, University College London, London WC1E 6BT, United Kingdom
[b] Old Dominion University, Norfolk, VA, USA
[c] Jet Propulsion Laboratory, California Institute of Technology, Pasadena, CA, USA
[d] Université Grenoble Alpes-CNRS, Grenoble, France
[e] MTA-ELTE Research Group on Complex Chemical Systems, Institute of Chemistry, Eötvös University, Budapest, Hungary
[f] Université de Reims Champagne-Ardenne, Reims, France
[g] University of Massachussets, Lowell, MA, USA
[h] National Institute of Standards and Technology, Gaithersburg, MD, USA
[i] Institute of Atmospheric Optics, Russian Academy of Sciences, Tomsk, Russia
[j] Harvard-Smithsonian Center for Astrophysics, Cambridge, MA, USA
[k] Institut d'Aéronomie Spatiale de Belgique, Brussels, Belgium
[l] Institute of Applied Physics, Russian Academy of Sciences, Nizhny Novgorod, Russia
[m] University of Science and Technology of China, Hefei, China

ARTICLE INFO

Article history:
Received 18 October 2013
Received in revised form
18 March 2014
Accepted 19 March 2014
Available online 28 March 2014

Keywords:
Water vapor
Transition wavenumbers
Atmospheric physics
Energy levels
Spectroscopic information system

ABSTRACT

This paper is the fourth of a series of papers reporting critically evaluated rotational–vibrational line positions, transition intensities, pressure dependences, and energy levels, with associated critically reviewed assignments and uncertainties, for all the main isotopologues of water. This paper presents energy level and transition data for the following doubly and triply substituted isotopologues of water: $D_2{}^{16}O$, $D_2{}^{17}O$, and $D_2{}^{18}O$. The MARVEL (Measured Active Rotational–Vibrational Energy Levels) procedure is used to determine the levels, the lines, and their self-consistent uncertainties for the spectral regions 0–14 016, 0–7969, and 0–9108 cm^{-1} for $D_2{}^{16}O$, $D_2{}^{17}O$, and $D_2{}^{18}O$, respectively. For $D_2{}^{16}O$, $D_2{}^{17}O$, and $D_2{}^{18}O$, 53 534, 600, and 12 167 lines are considered, respectively, from spectra recorded in absorption at room temperature and in emission at elevated temperatures. The number of validated energy levels is 12 269, 338, and 3351 for $D_2{}^{16}O$, $D_2{}^{17}O$, and $D_2{}^{18}O$, respectively. The energy levels have been checked against the ones determined, with an average accuracy of about 0.03 cm^{-1}, from variational rovibrational computations employing exact kinetic energy operators and an accurate potential energy surface. Furthermore, the rovibrational labels of the energy levels have been validated by

* Corresponding author.
E-mail address: j.tennyson@ucl.ac.uk (J. Tennyson).

http://dx.doi.org/10.1016/j.jqsrt.2014.03.019

an analysis of the computed wavefunctions using the rigid-rotor decomposition (RRD) scheme. The extensive list of MARVEL lines and levels obtained is deposited in the Supplementary Material of this paper, in a distributed information system applied to water, W@DIS, and on the official MARVEL website, where they can easily be retrieved.

1. Introduction

The first 13 authors of this paper formed a Task Group (TG) between 2004 and 2012 under the auspices of the International Union of Pure and Applied Chemistry (IUPAC) with the aim of constructing a database of water transitions from experiment and theory [1]. The individual tasks of the members of the TG are described in the first paper [2], henceforth mentioned as Part I, part of a series of manuscripts [1–4] published by the TG. Given the nature of water spectroscopy [5], the database built by the TG concentrates on the pure rotational as well as the rovibrational transitions of the water molecule corresponding solely to the ground electronic state.

In Part I [2], the TG derived energy levels and transition wavenumbers for the water isotopologues $H_2{}^{17}O$ and $H_2{}^{18}O$. In Part II [3], the isotopologues $HD^{16}O$, $HD^{17}O$, and $HD^{18}O$ were treated; improved data were also reported for $H_2{}^{17}O$ and $H_2{}^{18}O$, following the inclusion of several new sources in the analysis. In Part III [4], results obtained for the main water isotopologue, $H_2{}^{16}O$, were provided. All these studies utilized the Measured Active Rotational–Vibrational Energy Levels (MARVEL) protocol and code of Furtenbacher and Császár [6–9], which was extensively refined during Part III to allow for the treatment of large datasets. The results obtained by the IUPAC TG are reviewed in Ref. [1].

In the present work we apply the latest version of MARVEL [9] to the $D_2{}^{16}O$, $D_2{}^{17}O$, and $D_2{}^{18}O$ isotopologues of the water molecule. $D_2{}^{16}O$, doubly deuterated (heavy) water, has a fractional abundance in Earth's atmosphere, compared to $H_2{}^{16}O$, of about 20 parts per billion (ppb). As a trace species, $D_2{}^{16}O$ is currently not represented in the main atmospheric databases [10,11]. Nevertheless, atmospheric absorption by $D_2{}^{16}O$ is of significance. The reason is that the absorption spectrum of $D_2{}^{16}O$ is substantially shifted from both the main isotopologue, $H_2{}^{16}O$, and that of $HD^{16}O$. Furthermore, even with its highly reduced atmospheric concentration compared to $H_2{}^{16}O$, $D_2{}^{16}O$ still has absorption features which lie above the cut-off for water lines adopted by HITRAN [10].

Fundamental equations of state for the whole field of liquid and vapor states of water, including heavy water, from the triple point up to 800 K and 100 MPa have been of interest to the scientific and engineering communities for quite some time [12–16]. At present heavy water is not one of the species adopted by the International Association for the Properties of Water and Steam (IAPWS) in their 1995 formulation of the thermodynamic properties of ordinary water substance for general and scientific use [16]. Nevertheless, an IAPWS release from 2005 [17] and a background paper [14] do prove the importance of the thermochemical properties of heavy water, including those of its vapor. The IAPWS steam tables are widely used and the high-temperature partition function of $D_2{}^{16}O$ employed in these tables is significantly less studied, and therefore more uncertain, than other key parameters in the IAPWS formulation. Results of the present study can be used to remedy this situation.

$D_2{}^{16}O$ is thought to be particularly important for checking emissions in the region of nuclear power plants, and monitoring protocols based on spectroscopic methods are being discussed [18]. Astronomical observations of $D_2{}^{16}O$ are also important. Some environments, most notably Venus [19,20], have heavily enhanced D/H ratios making deuterated water isotopologues much more significant. Measurement of the D/H ratio is important to test chemical evolution models of the galaxy. According to present theories of primordial nucleosynthesis, deuterium was formed in the first few minutes after the Big Bang. As D is destroyed rapidly by nuclear reactions in stellar interiors, the abundance of D has been reducing ever since. At cold temperatures, below 20 K, the difference in the binding energy of H_2O, HDO, and D_2O becomes significant and leads to much higher abundances of deuterated molecules than the standard D/H ratio would suggest [21,22]. The chemistry of carbon-containing molecules also contributes to the overabundance of deuterated molecules. Consideration of deuterated molecules is necessary when establishing the budget of the available deuterium. Thus, doubly [23] and triply deuterated [24,25] ammonia has been found in cold dark clouds, as well as doubly deuterated D_2H^+ [26], D_2S [27], D_2CO [28], D_2CS [29], and c-C_3D_2 [30]. Heavy water has also been detected in the interstellar medium [22,31–33].

Finally, we note that D_2O is often used in laboratory experiments for technical reasons as a proxy for H_2O, as the heavier mass of D can make discrimination easier. Examples of this usage include extensive work on the D_2O dimer [34], and work on energy deposition in D_2O following dissociative recombination of D_3O^+ [35]. The latter study, among other things, helps us to address the issues raised by the detection of non-thermal $H_2{}^{16}O$ emission in comets [36]. Work on water lasers provides another example. The original, serendipitous discovery of water emissions in a discharge occurred for $H_2{}^{16}O$ [37]. However, high-resolution observations of emissions from such a source are only available for $D_2{}^{16}O$ [38]. All these examples require detailed information on the rovibrational energy level structure of D_2O.

As emphasized already in Part I, a distinguishing feature of the present series of IUPAC-sponsored studies

Table 1
Data sources and their characteristics for $D_2{}^{16}O$. See Section 2.1 for comments.[a]

Tag	Range (cm^{-1})	Trans. A/V	MUI	MAD	Physical conditions					Comments
					T (K)	p (hPa)	Abun.	Rec.	L (m)	
53Crawford [58]	0.296	1/1	5	0.3	RT		100	SMM	3	(1a)
54PoSt [60]	0.364–0.365	2/2	1	0.2	RT			MW	0.9,3	(1b)
70BeClFrSu [67]	0.364–20.26	28/28	10	1	RT					(1c)
84MeLuHe [80]	0.364–35.53	88/88	10	6	RT		100		1	(1d)
07BrMuEnLe [111]	0.364–91.10	161/161	100	41	RT,346		100,50	FTS/BWO		
85Johns [82]	0.364–220.1	265/265	200	93	RT	< 2.66		FTS	2.46	(1e)
68VeBlDy [66]	0.365	1/1	5	4				BMS		(1f)
70StBe [69]	0.991–20.26	28/28	6	2	RT			MW		
53JeBiMa [59]	1.007–1.027	2/2	2	0.1			100	MW		
56ErCo [63]	1.448–3.114	3/3	7	2	RT			MW		
10CaDoPuGa [118]	3.114–13.46	13/13	0.04	0.00						
70BeSt [68]	4.841–7.196	4/4	150	101	RT			MW		
87BaAlAlPo [84]	10.08–15.94	14/14	4500	2613						
76FlGi [74]	10.57–39.86	36/33	4100	3239	RT	13.3–18.7	100,50	FS	0.203	(1g)
70StSt [70]	18.52–20.26	2/2	2500	2458		0.027		BWO	0.15	
01MaMaQiOh [101]	18.52–171.6	157/157	20	4	RT	< 0.0013	99.75	MW	1.5	
13CaPu [120]	34.80–39.86	7/7	0.05	0.00						(1h)
01MiKeAnSa [38]	49.18–74.11	117/113	100	76	RT					
95PaHo [93]	110.6–413.8	215/214	114	102	RT	0.5	50	FTS	3.2	(1i)
04MeMiStTa [105]	322.0–1658	1153/1152	944	471	1520–1950	1.0–16.0	100	FTS	1	(1j)
05MiMeStTa [107]	322.2–3398	3539/3515	2454	1620	1940	10.6	100	FTS	1	(1k)
06ZoOvShPo [110]	380.1–4315	25 311/24 808	4987	3688	1823	26.66		FTS	1	(1l)
99Tothb [96]	864.2–1731	784/784	202	141	296	0.66–6.83	14.6–50.6	FTS	≤ 433	(1m)
93Tothc [91]	913.5–1572	940/940	303	198	297	0.77–21.2	18.1–89.7	FTS	0.25–2.39	(1n)
91RiSmDeBe [87]	1017–1428	135/134	313	239	294–297	≤ 1.3		FTS	1.21	(1o)
85CaFlMaGu [81]	1039–1585	838/838	530	324	RT	0.20–2.17	100	FTS	40.2	(1p)
86ThRiSmBe [83]	1073–1272	17/16	318	230	RT	0.07–2.0	100	L	0.5	(1q)
81PaFlCaGu [77]	2172–3089	1648/1648	793	629	296	0.33–1.35	100	FTS	20–60	(1r)
92RiSmDeBe [89]	2657–2725	8/8	467	191	295–297	≤ 1.3		FTS	1.21	(1s)
00ByNaSiVo [97]	3286–3641	347/344	697	483	300	0.1–12	50	FTS	240	
00HeUlOnBe [98]	3322–4161	1082/1082	1000	758	RT	0.33–16.5	25–98	FTS	15–105	
00WaUlOnBe [100]	4779–5719	1762/1759	2000	1956	RT	1.13–15.4	25–98	FTS	15–105	
14LiNaKaCa [121]	5855–6802	2781/2780	1611	1684	RT	1.31, 13.1	25	CRDS		
93OrRaWiWi [90]	6030–6881	1656/1631	1871	1251	RT	0.21–21.2	100	FTS	240	(1t)
12MiNaNiVa [119]	6056–9122	1438/1438	2760	2361	RT	19.35	O^{18} Enr.	FTS	105	
94ByNaSiWi [92]	6373–6611	98/95	1895	1489	RT	5.8	100	FTS	240	(1u)
89OhSa [86]	6384–6601	330/323	6718	3912	RT	10.67	50	L		(1v)
91SaTaIrNa [88]	6564–6564	1/1	10	0.1	RT	12.67	100	L	1.0	(1w)
10ByNaPoHu [117]	7366–8434	2772/2764	2193	1772	RT	20.5	100	FTS	15–87	
00UlHeOnBe [99]	7629–8048	6/4	2000	2012	RT	10.9–15	25–75	FTS	15–69	(1z)
96CoBaRo [94]	7779–7989	94/81	15 247	14 012	RT	26.66	Pure	PAS		(1aa)
06NaLeShJe [108]	8800–9538	1410/1408	5927	2819	RT	2.6–18.2	99.9	FTS	600	
01ZhUlOnBe [103]	8835–9166	277/277	2259	1787	RT	16.0	99.8	FTS	105	(1bb)
82ByLoMaSi [78]	9163–9539	65/0			RT	16.0	99.8	FTS	105	(1cc)
01UlHuBeOnb [102]	10 189–10 440	216/214			RT	23.5/10.7	99.8	FTS	105/15	
07NaMaLeTe [113]	11 402–11 908	956/954			RT	20	99.96	ICLAS	14 400	
07CaMaBePo [112]	12 485–12 853	1261/1254	8783	4893	RT	20	99.96	ICLAS	14 400	(1dd)
02HuUlBeOn [104]	12 552–12 811	187/177	5510	7333	RT	12	99.8	ICLAS	19 000	(1ee)
08NaLeBeCa [114]	12 849–13 375	996/995	7176	7807	RT	18.4	99.96	ICLAS	24 000	
09CaLeNa [115]	13 604–14 016	282/282			RT	18.4	99.96	ICLAS	24 000	

[a] The tags listed are used to identify experimental data sources throughout this paper. The range given represents the range corresponding to wavenumber entries within the MARVEL input file and not the range covered by the relevant experiment. Uncertainties of the individual lines can be obtained from the Supplementary Material. Trans. = transitions, with A = number of assigned transitions in the original paper, V = number of transitions validated in this study. MUI = mean uncertainty of the transitions inputed from a given source and entering the MARVEL analysis in units of 10^{-6} cm^{-1}; MAD = median absolute deviation of the residuals in units of 10^{-6} cm^{-1}, only those residuals were considered where both the upper and the lower energy levels were determined by at least three different sources. T = temperature (K), given explicitly when available from the original publication, with RT = room temperature and NLTE is non-local thermodynamic equilibrium. p = pressure (hPa). Abun. = abundance (%) of the given isotopologue in the gas mixture, with Enr = enriched and Nat = natural abundance. Rec. = experimental technique used for the recording of the spectrum, with SMM = Stark-modulated microwave spectrometer, BWO = backward wave oscillator, FTS = Fourier transform spectroscopy, L = different lasers, and MW = microwave spectrometer, PAS = photo-acoustic spectrometer, CRDS = cavity ring-down spectroscopy.

is the joint utilization of all available experimental and the best theoretical transition wavenumber and energy-level data, with a long-term aim to create a complete linelist for all water isotopologues. Obtaining a complete linelist is outside the scope of present-day experiments, but in general it can be determined by means of sophisticated

Table 2
Experimental data sources and their characteristics for $D_2{}^{17}O$. See Section 2.2 for comments.[a]

Tag	Range (cm^{-1})	Trans. A/V	Physical conditions					Comments
			T (K)	p (hPa)	Abun.	Rec.	L (m)	
73BeLaSt [123]	0.71–13.33	19/16	RT	0.03–0.4		MW		(2a)
12PuCaGa [122]	7.89–53.35	49/47	RT		50	FMSS		(2b)
99Tothb [96]	996.0–1389.4	221/213	RT	0.003–0.04		FTS	≤ 433	(2c)
12MiNaNiVa [119]	6166.4–7968.6	277/273	RT	19.35		FTS	105	
14LiNaKaCa [121]	6379.9–6620.0	34/34	RT	1.31, 13.1	25	CRDS		

[a] See footnote a in Table 1.

first-principles computations. Consequently, as long as experiments have a higher precision than even the most advanced computations that can be performed for a molecule of the size of water, the complete linelist will necessarily contain a combination of accurate experimental data and less accurate predicted data. MARVEL-type efforts help us to (a) replace as many computed line positions with their experimental counterparts as possible, (b) reduce the uncertainty, under ideal circumstances, with which a transition has been determined, and (c) propose labels for the assignment of absorption and emission spectra.

2. Methods and input data

The methods employed in this study for collecting and critically evaluating experimental transition wavenumbers and uncertainties and for inverting the wavenumbers in order to obtain the best possible energy levels along with their uncertainties are based on the MARVEL procedure [6–9], which is built upon the theory of spectroscopic networks (SNs) [39–41] and involves an iterative robust reweighting scheme [42]. During a MARVEL analysis we simultaneously process all the available assigned experimental lines and the associated energy levels for the chosen isotopologue. The reweighting scheme means that uncertainties for the selected transitions are changed (increased) during iterations of the MARVEL procedure until self-consistency within the given dataset is achieved.

The first step in the MARVEL procedure is to split the transition data into components of the SN created from the observed data. Components of the SN contain all interconnecting rotational–vibrational energy levels supported by the grand database of the transitions. D_2O has ortho and para nuclear-spin states that are not interconnected spectroscopically [43]. Therefore, the observed transitions form two principal components (PCs) which must be linked by a so-called magic number in order to have absolute energies for levels in both PCs. Interconnected transitions or even single transitions unattached to the rooted PCs are part of floating components (FCs); such transitions can in principle be linked to the PCs but only with new observational data. After cleansing of the available data and applying the iterative robust reweighting algorithm for the chosen components, a database is created containing self-consistent and correctly assigned transitions and having the lowest possible related uncertainties. Energy levels, and their uncertainties, determined from these transitions are in harmony with the measured transitions and their (adjusted) uncertainties.

The rovibrational spectrum of $D_2{}^{16}O$ has been investigated by a considerable number of experimental studies [38,44–121]. In particular, we note that a number of emission studies of hot $D_2{}^{16}O$ spectra [105–107,110] are included in the above list. Hot spectra are usually considerably richer in transitions but have significantly larger uncertainties and a higher chance of misassignment (and/or mislabeling) than spectra recorded at room temperature. As expected, there is a much smaller number of publications reporting measured transitions for $D_2{}^{17}O$ [96,119,121–123] and $D_2{}^{18}O$ [74,82,91,119,121,123–130]. There are also a number of theoretical and computational studies on the energy levels and transitions of D_2O isotopologues, including some less [131] and some more [132–135] advanced ones.

For each data source, Tables 1–3 provide experimental information related to the spectra of $D_2{}^{16}O$, $D_2{}^{17}O$, and $D_2{}^{18}O$, respectively. The number of originally measured and validated transitions for each data source is given there, as well. To be included in our tabulation, data sources must provide original experimental line positions with assignments and uncertainties. The mean uncertainty of the transitions inputed (MUI) from a given source and entering the MARVEL analysis is given in Tables 1 and 3, in units of 10^{-6} cm^{-1}, for $D_2{}^{16}O$ and $D_2{}^{18}O$, respectively. The same tables also show median absolute deviations (MADs) of the transition residuals, observed – MARVEL, in units of 10^{-6} cm^{-1}. Only those residuals were considered when computing the MAD values where both the upper and the lower energy levels were determined by at least three different sources. Comparison of the MUI and MAD values indicates for each source how reasonable the input uncertainties are in light of all the other data sources. Such comparisons helped to input more accurate uncertainties in cases where the uncertainties of the measured transitions were not explicitly given in the original source. The experimental conditions of the measurements are summarized in the columns 'Physical conditions' in the tables. Each data source is identified with a tag. As specified in Part I, the tag is based on the year of publication and the names of the authors.

Most of the spectra were obtained by Fourier transform spectroscopy (FTS), which provides a wide spectral coverage from the far infrared region to the near ultraviolet. In order to detect weak lines, FTS spectrometers have been equipped with long multipass cells. The CRDS

Table 3
Experimental data sources and their characteristics for $D_2{}^{18}O$. The number of transitions in floating components is 57. See Section 2.3 for comments.[a]

Tag	Range (cm^{-1})	Trans. A/V	MUI	MAD	Physical conditions					Comments
					T (K)	p (hPa)	Abun.	Rec.	L (m)	
85Johns [82]	0.30–216.37	144/144	500	253	RT	< 2.66		FTS	2.46	(3a)
73BeLaSt [123]	0.30–12.56	21/21	1000	887	RT	0.03–0.4		MW		(3b)
76FlGi [74]	19.88–38.15	15/12	7692	7735	RT	13.3–18.7	90% ^{18}O	0.2		(3c)
96WaTaTaOn [125]	921.3–1713.7	62/32	5000	7038	296	0.4–0.7	31.6	FTS	0.2	(3d)
93Tothc [91]	953.3–1301.4	439/439	500	237	297	0.8–21.2	2.2–10.2	FTS		
89LoFu [124]	964.9–1443.5	614/611	648	532	274–279			FTS	1.24	(3e)
11LiSoNiHu [126]	969.1–1605.5	1155/1152	500	217	RT	0.38–15.2	98% ^{18}O	FTS	15	(3f)
08NiLiSoHu [127]	2088.5–3217.7	3878/3836			296–298	0.6–19.4	98% ^{18}O	FTS	15–105	(3g)
05Toth [128]	2594.5–2917.3	298/286			296		≤ 10.2	FTS	2.39	(3h)
14LiNaKaCa [121]	5973.0–6778.7	503/503			RT	1.31, 13.1	25	CRDS		
12MiNaNiVa [119]	6002.6–9108.4	4537/4520	2193	1488	297	19.35	73.7	FTS	105	(3i)
10MiTaDaJe [129]	6127.3–8245.6	286/286	5280	2611	290–293			FTS	600	(3j)
12DoTeOrCh [130]	6328.0–6637.6	194/160	7619	3519	296		9.3	IBBCEAS	33–370	(3k)

[a] IBBCEAS: Incoherent Broadband Cavity-Enhanced Absorption Spectroscopy; otherwise see footnote a in Table 1.

(cavity ringdown spectroscopy) and ICLAS (intracavity laser absorption spectroscopy) techniques are limited to certain spectral regions depending on the availability of tunable laser sources. These techniques have specific advantages in terms of sensitivity and spectral resolution, which make them particularly suitable for the characterization of spectral regions with weak absorption features.

As an independent validation of the experimental transition wavenumbers and the derived energy levels, systematic comparisons were made with results from state-of-the-art variational nuclear-motion computations. For this purpose, a computed $D_2{}^{16}O$ linelist, due to Shirin and co-workers [135], was employed. This linelist, containing transitions between 0 and 16 000 cm^{-1} and up to $J=30$, is notable for its accuracy: it reproduced the levels available at the time of its construction for $J=0,2,5$, and 10 with a standard deviation of only 0.023 cm^{-1}(J is the rotational quantum number). Consequently, any MARVEL level obtained for the D_2O isotopologues as part of this work which differed by more than 0.1 cm^{-1} from its variational counterpart was subject to further scrutiny. For transitions removed at this stage, see the appropriate comments in the footnotes of Tables 1–3 and especially the Supplementary Material.

We require that the resulting dataset contains unique labels both for the lower and the upper states involved in the transitions. We retain the order of the vibrational labels found for $H_2{}^{16}O$ for the D_2O isotopologues, *i.e.*, v_1, v_2, and v_3 stand for the symmetric OD stretching, bending, and the antisymmetric OD stretching quantum numbers, respectively. We use the standard asymmetric-top quantum numbers $[JK_aK_c] \equiv J_{K_aK_c}$ to label the rotational states. Thus, the rotation–vibration levels of each isotopologue are identified uniquely by six labels altogether. Finally, we note that, as deuterium is a boson, compared to H_2O, the ortho and para states are swapped in D_2O. For D_2O, states for which $(K_a+K_c+v_3)$ is even are called ortho with a degeneracy of 12, and the odd states are called para with a degeneracy of 6.

The rigid-rotor decomposition (RRD) scheme [136,137] was employed to check the rotational-energy-level labels. The labels are based on RRD tables formed by projecting rotational–vibrational ($J \neq 0$) wavefunctions onto products of symmetrized rigid-rotor basis functions and previously computed ($J=0$) vibrational eigenstates. As previous studies indicate [137], in the case of water isotopologues the quantum numbers J, K_a, and K_c can be determined without ambiguity for lower energies and J values, principally up to the barrier to linearity, *i.e.*, close to about 11 000 cm^{-1} [138–140].

2.1. Comments on the data sources for $D_2{}^{16}O$ given in Table 1

(1a) 53Crawford [58]: Two new spectral lines, one for $D_2{}^{16}O$ and one for $HD^{16}O$, were observed in this study using a Stark modulated spectrometer.

(1b) 54PoSt [60]: In this early work the emphasis was on the spectrum of the HDO molecule. Only two $D_2{}^{16}O$ transitions were found.

(1c) 70BeClFrSu [67]: Reports 29 MW transitions observed using a harmonic generator, but one comes from 70BeSt [68].

(1d) 84MeLuHe [80]: Millimeter- and submillimeter-wave measurements of $H_2{}^{16}O$, $HD^{16}O$, and $D_2{}^{16}O$ obtained in the region 300–1100 GHz. The spectra were recorded with a high-resolution spectrometer equipped with a 1.5 K InSb detector.

(1e) 85Johns [82]: Absorption spectra of six water isotopologues, recorded with a Bomem DA 3.002 Fourier transform spectrometer with a maximum optical path difference (MOPD) of 246 cm, were reported. The average accuracy of the measurements estimated by the author is 0.0002 cm^{-1}. The stainless-steel sample cell was 15 cm long and was fitted with high-density polyethylene windows. The sample pressure was less than 1 Torr so as to minimize possible pressure shifts and pressure broadenings. In the case of wavenumbers below 30 cm^{-1} the sample pressure was 2 Torr. HF and HCl lines measured by Jennings et al. [141] were employed for calibration. A few H_2O lines below 33 cm^{-1} measured by Helminger et al. [142] and one HCl line measured by De Lucia et al.

Table 4
Recalibration factors determined during the present study for four data sources reporting $D_2{}^{16}O$ transitions in a given wavenumber range.

Source	Range (cm^{-1})	Recalibration factor
85CaFlMaGu [81]	1039–1585	1.00000008
93OrRaWiWi [90]	6030–6881	0.99999982
94ByNaSiWi [92]	6373–6611	0.99999985
89OhSa [86]	6384–6601	0.99999980

[143] using the microwave technique were also used for calibration.

(1f) 68VeBlDy [66]: Hyperfine structure measurements were obtained using beam maser spectroscopy.

(1g) 76FlGi [74]: Far-infrared absorption spectra of six water isotopologues were observed between 10 and 40 cm^{-1} at a resolution of 0.07 cm^{-1}. The spectra were recorded with a NPL-Grubb Parsons Cube interferometer equipped with a liquid helium cooled Rollin-type InSb detector.

(1h) 13CaPu [120]: Reports the results of the most accurate measurements on heavy water, with an accuracy of 1 kHz in the THz region. The two sets of transitions where the hyperfine structure was resolved were deperturbed for the present analysis by Puzzarini.

(1i) 95PaHo [93]: The pure rotational spectra of H_2O, HDO and D_2O were measured to obtain line positions for calibration purposes. The spectra were recorded with a Bruker IFS 120 HR Fourier-transform spectrometer. A White-type cell that gives an absorption path length of 3.2 m was filled with a mixture of $H_2{}^{16}O$, $HD^{16}O$, and $D_2{}^{16}O$ at room temperature to a total pressure of 0.5 hPa, and then 0.5 hPa of OCS was added for calibration. Partial pressures were not estimated due to a residual amount of natural water present in the cell.

(1j) 04MeMiStTa [105]: Far-infrared emission spectra measured at different temperatures at a resolution of 0.0055 cm^{-1}. The measurements were performed in an aluminum cell with an effective length of hot gas of about 50 cm. Transitions between highly excited rotational levels are reported, with J_{max} equal to 26 and 25 for the (0 0 0) and (0 1 0) vibrational states, respectively.

(1k) 05MiMeStTa [107]: The following label changes had to be performed to conform with other MARVEL transitions and the results of variational nuclear-motion computations: (1 0 0)11_{74} and (1 0 0)11_{75} were exchanged with (0 0 1)11_{66} and (0 0 1)11_{65}, respectively. Furthermore, (0 0 1)$18_{6,13}$ was changed to (1 0 0)$18_{7,11}$, (1 0 0)$16_{13,3}$ to (0 2 0)$16_{13,3}$, and (0 2 0)$16_{13,3}$ to (1 2 0)$16_{13,3}$.

(1l) 06ZoOvShPo [110]: This source contains almost half of the assigned and measured transitions of $D_2{}^{16}O$, including those reported first in 04ShZoPoTe [106]. 35 relabelings had to be performed to conform with other MARVEL transitions and the results of variational nuclear-motion computations.

(1m) 99Tothb [96]: This work is the continuation of an earlier work from the same author [144]. The linestrengths of the hot bands of $D_2{}^{16}O$, (020)–(010), (100)–(010), and (001)–(010), were analyzed using a full perturbation treatment.

(1n) 93Tothc [91]: $D_2{}^{16}O$ and $D_2{}^{18}O$ transitions in the ν_2 band were reported with a resolution of 5×10^{-3} cm^{-1}. This work is the continuation of the study of the ν_2 bands of the $H_2{}^{16}O$, $H_2{}^{17}O$, $H_2{}^{18}O$, $HD^{16}O$, $HD^{17}O$, and $HD^{18}O$ molecules. The paper states that the wavenumbers reported in 85CaFlMaGu [81] differ on average by 0.0002 cm^{-1} from the correct values due to a calibration problem.

(1o) 91RiSmDeBe [87]: Determination of room temperature Lorentz-broadening and pressure-induced line-shift coefficients in air, nitrogen, and oxygen. Twelve spectra were analyzed to determine ν_2 $D_2{}^{16}O$ lines. The measurements were recorded with the FTS of the Kitt Peak National Observatory at 0.0053 cm^{-1} resolution. Gas samples were prepared by mixing distilled H_2O with 99.96 mol% D_2O. To measure accurate zero-pressure line center positions for the determination of the pressure shift coefficients a low pressure ($\leq$1.0 Torr) spectrum of each mixture was recorded. For the broadening and shift measurements, the low pressure samples were diluted with high purity nitrogen, oxygen, or ultra-zero air at total sample pressures of 200, 300, and 400 Torr. The total H_2O + HDO + D_2O volume mixing ratio was about 0.3% in the mixtures.

(1p) 85CaFlMaGu [81]: Four Fourier-transform spectra are reported, the estimated accuracy of the line positions is 4×10^{-4} cm^{-1}. The transitions were recalibrated during the present study, see Table 4 for the recalibration factor employed.

(1q) 86ThRiSmBe [83]: Absolute line intensity measurements in the ν_2 bands of HDO and D_2O using a tunable diode laser spectrometer were reported. 50 cm absorption path Pyrex cell fitted with teflon valves and wedged potassium chloride windows was used. For the D_2O measurements, pure (99.5 mol%) D_2O was used.

(1r) 81PaFlCaGu [77]: Analysis of the (0 0 0), (0 2 0), (1 0 0), and (0 0 1) vibrational states up to $J=19$ and $K_a=10$ was reported. The three analyzed spectra were recorded with a resolution of about 5×10^{-3} cm^{-1}. The authors previously studied the corresponding $2\nu_2$, ν_1, and ν_3 bands of $H_2{}^{16}O$ and in this paper report the first analysis of the $2\nu_2$ band of $D_2{}^{16}O$.

(1s) 92RiSmDeBe [89]: The high-resolution Fourier-transform spectrometer of the Kitt Peak National Observatory was used to determine Lorentz-broadening coefficients and pressure-induced line-shift coefficients with a resolution of 0.0053 cm^{-1}. A sample cell with potassium chloride windows was used for the measurements. The detectors were two liquid-He-cooled As-doped Si photoconductors. The signal to noise ratio was 200 at 2600 cm^{-1}, which decreased to 100 at 2725 cm^{-1}. Gas samples were prepared by mixing distilled H_2O with 99.96 % D_2O. Low pressure ($\leq$1.0 Torr) samples were mixed with samples diluted with high-purity N_2, O_2, or ultra-zero air at total sample pressures of about 200, 300, and 400 Torr.

(1t) 93OrRaWiWi [90]: The assigned transitions belong to the $3\nu_2+\nu_3$, $\nu_1+\nu_2+\nu_3$, $\nu_1+3\nu_2$, 2 $\nu_1+\nu_2$, and $\nu_2+\nu_3$ bands of $D_2{}^{16}O$. The transitions were recalibrated during the present study, see Table 4 for the recalibration factor employed.

(1u) 94ByNaSiWi [92]: Weak lines were studied between 6000 and 7000 cm^{-1}. $\nu_1+2\nu_2+\nu_3-\nu_2$ is the first hot band found in the infrared spectrum of D_2O. The authors analyzed the unidentified weak lines reported by 93OrRaWiWi [90]. A Bruker IFS 120 HR interferometer, working in Giessen, Germany, was employed, equipped with a 4 m base length White-type cell adjusted for 240 m total path length. One label was changed, (1 2 1)5_{42} to (1 2 1)5_{32}. The transitions were recalibrated during the present study, see Table 4 for the recalibration factor employed.

(1v) 89OhSa [86]: Absorption spectra of HDO and D_2O were measured using seven single-mode distributed feedback (DFB) semiconductor lasers. The $\nu_1+\nu_3$ band of HDO and the $\nu_1+\nu_2+\nu_3$ and 2 $\nu_1+\nu_2$ bands of D_2O in the range 6380–6600 cm^{-1} were reported. The transmitted radiation was detected by a germanium photodiode. For the D_2O measurements the absorption cell was filled with a mixture of H_2O and D_2O (in ratio 1:1) at a total pressure of 8 Torr. Two labels were changed, (2 1 0)8_{17} to (0 1 2)8_{17} and (2 1 0)8_{53} to (0 1 2)8_{17}. The transitions were recalibrated during the present study, see Table 4 for the recalibration factor employed.

(1w) 91SaTaIrNa [88]: One transition of D_2O was measured using a near-infrared semiconductor-laser spectrometer. As to frequency calibration, the InGaAsP semi-conductor laser was heterodyned with a Lamb-dip-stabilized 1.52 μm ^3He–^{20}Ne laser. The authors used a 1-m long absorption cell and a 1:1 mixture of H_2O and D_2O at a pressure of 9.5 Torr for D_2O.

(1z) 00UlHeOnBe [99]: One label (0 2 2)8_{45} was changed to (3 0 0)8_{45}.

(1aa) 96CoBaRo [94]: Photoacoustic laser absorption spectroscopy was employed to measure (2 0 1)←(0 0 0) rovibrational transitions with a resolution of 0.07 cm^{-1}. D_2O was prepared in the excited state by IR excitation using the Raman shifted output of a Nd:YAG dye laser.

(1bb) 01ZhUlOnBe [103]: One label exchange, (2 1 1)4_{22} and (3 1 0)4_{32}, and one label change, (2 1 1)10_{47} to (1 1 2) 10_{19}, were performed.

(1cc) 82ByLoMaSi [78]: A Nd intracavity laser spectrometer was used to obtain spectra of H_2, HDO, and D_2O in the 9161.5–9392.5 cm^{-1} spectral region. The $\nu_2+3\nu_3$ and the $\nu_1+\nu_2+2\nu_3$ bands of $D_2{}^{16}O$ were analyzed. The absorption sensitivity was 10^{-7} cm^{-1}. The accuracy of the line center determination was 0.08 cm^{-1}. None of the lines of this study could be validated.

(1dd) 07CaMaBePo [112]: One label change, from (2 2 2)7_{25} to (5 0 0)7_{43}, was made.

(1ee) 02HuUlBeOn [104]: Two label changes, (4 0 1)2_{02} to (5 0 0)2_{12} and (4 0 1)9_{09} to (1 4 2)9_{37}, were made to conform with other transitions.

2.2. Comments on the data sources for $D_2{}^{17}O$ given in Table 2

(2a) 73BeLaSt [123]: The first measurement of the microwave spectrum of $D_2{}^{17}O$ and $D_2{}^{18}O$, between 8 and 400 GHz, recorded in two mixtures: (a) 93% $D_2{}^{18}O$ and 0.6% $D_2{}^{17}O$, and (b) 14% $D_2{}^{18}O$ and 60 % $D_2{}^{17}O$. Pure rotational transitions are reported for J=1–9. The hyperfine structure of the lines is resolved but not taken into account during the present analysis.

(2b) 12PuCaGa [122]: Measurements extended up to the THz region recorded in a equal mixture of $D_2{}^{17}O$ and $H_2{}^{17}O$. The hyperfine structure of the lines was resolved but is not taken into account during the present analysis.

(2c) 99Tothb [96]: Continuation of a previous research project [144]. The first detection of the ν_2 band of $D_2{}^{17}O$.

2.3. Comments on the data sources for $D_2{}^{18}O$ given in Table 3

(3a) 85Johns [82]: 165 pure rotational transitions in the far-IR region are reported in this source, of which 21 were taken from 73BeLaSt [123]; we considered these transitions as belonging to the original source.

(3b) 73BeLaSt [123]: The experimental conditions are exactly the same as for $D_2{}^{17}O$. See also note (2a).

(3c) 76FlGi [74]: Six water isotopologues, $H_2{}^{16}O$, $HD^{16}O$, $D_2{}^{16}O$, $D_2{}^{18}O$, $H_2{}^{18}O$, and $HD^{18}O$, are treated in this source, see Parts I–III for further details.

(3d) 96WaTaTaOn [125]: Of the transitions reported in this source, 12 transitions belong to floating components. Several energy levels involved in the transitions reported have no variational counterparts within a given symmetry and 0.1 cm^{-1}.

(3e) 89LoFu [124]: The three deleted transitions could not be verified by the present MARVEL database.

(3f) 11LiSoNiHu [126]: The three unvalidated transitions belong to floating components.

(3g) 08NiLiSoHu [127]: The transitions belong to the (0 0 1), (1 0 0), and (0 2 0) vibrational states. 20 transitions belong to floating components of the SN and thus could not be validated. Several transitions involve energy levels which do not have variational counterparts within a given symmetry and 0.1 cm^{-1}.

(3h) 05Toth [128]: 12 transitions had to be deleted during the MARVEL analysis.

(3i) 12MiNaNiVa [119]: One transition from this source forms a floating component and thus could not be validated. 34 transitions were deleted as they involve upper energy levels which do not have variational counterparts within a given symmetry and a 0.1 cm^{-1} window.

(3j) 10MiTaDaJe [129]: The first source reporting transitions beyond 3200 cm^{-1} for $D_2{}^{18}O$.

(3k) 12DoTeOrCh [130]: An analysis of previous, unassigned measurements by 08OrRu [145], who recorded a spectrum using water enhanced in both D and ^{18}O is presented. 12DoTeOrCh contains 33 partially assigned transitions labeled in the original source as “BT2”. One further transition had to be deleted as it involves an energy level which has no variational counterpart within a given symmetry and a 0.1 cm^{-1} window.

2.4. Recalibrations

The experimental line positions utilized in this study for the three D_2O isotopologues have been measured over several decades under widely different experimental conditions, including pressure and temperature differences, and different apparatus. When these data are combined,

Table 5
MARVEL vibrational band origins (VBOs) for $D_2{}^{16}O$, with normal-mode ($v_1v_2v_3$) labels, MARVEL uncertainties (Unc.), and the number of rotational levels (RL) associated with the vibrational levels in the present database. [a]

P	$v_1v_2v_3$	VBO/cm^{-1}	Unc.	RL	P	$v_1v_2v_3$	VBO/cm^{-1}	Unc.	RL
0	0 0 0	0.000000[b]	0	849	8	2 2 1	[10 180.1]		8
1	0 1 0	1178.378792	200	813		4 0 0	[10 341.0]		6
2	0 2 0	2336.838866	384	702		3 0 1	10 358.563019	1000	89
	1 0 0	2671.645857	396	683	9	3 3 0	[11 245.7]		5
	0 0 1	2787.717995	385	757		2 3 1	[11 289.7]		9
3	0 3 0	3474.319300	790	556		1 3 2	[11 441.2]		18
	1 1 0	[3841.4]		479		0 3 3	[11 605.8]		45
	0 1 1	3956.007487	3113	605		4 1 0	11 483.639200	5000	85
4	0 4 0	[4589.3]		271		3 1 1	11 500.247519	5000	160
	1 2 0	4990.827612	1919	197		2 1 2	11 679.389300	5000	94
	0 2 1	5105.384472	1822	396		1 1 3	11 816.636619	5000	114
	2 0 0	5291.721700	2000	196	10	2 4 1	[12 378.5]		9
	1 0 1	5373.902132	1951	295		1 4 2	[12 530.8]		29
	0 0 2	5529.437629	2500	339		0 4 3	[12 698.5]		24
5	0 5 0	[5679.6]		61		4 2 0	[12 603.6]		34
	1 3 0	6119.024000	1500	168		3 2 1	12 618.912019	7000	164
	0 3 1	6235.080620	976	304		2 2 2	[12 799.1]		45
	2 1 0	6452.979058	1500	194		1 2 3	[12 934.1]		96
	1 1 1	6533.235231	1246	268		0 2 4	[13 112.1]		1
	0 1 2	6687.001534	1486	249		5 0 0	12 737.397000	7000	115
6	*0 6 0*	[6742.1]		0		4 0 1	12 743.024424	4069	161
	1 4 0	[7224.7]		38		3 0 2	12 988.432800	1000	112
	0 4 1	[7343.9]		195		2 0 3	13 088.307419	1000	146
	2 2 0	7593.267100	1800	104		1 0 4	13 263.902600	1000	61
	1 2 1	7672.923419	1800	184	11	0 9 1	[12 473.1]		1
	0 2 2	[7826.3]		131		4 3 0	[13 702.6]		2
	3 0 0	7852.929271	1461	174		3 3 1	13 717.264519	1000	44
	2 0 1	7899.825330	1454	217		2 3 2	[13 900.3]		1
	1 0 2	8054.074100	1800	152		1 3 3	[14 033.4]		4
	0 0 3	8220.178195	1461	203		4 1 1	13 876.020819	1000	90
7	2 3 0	[8712.1]		11		3 1 2	[13 869.4]		36
	1 3 1	[8792.7]		82					
	0 3 2	[8947.0]		14					
	3 1 0	[9005.5]		102					
	2 1 1	9050.349119	5000	176					
	1 1 2	9202.716000	5000	139					
	0 1 3	9366.313119	5000	157					

[a] The VBOs are grouped by polyad number P defined as $P=2v_1+v_2+2v_3$. All VBOs are listed up to $P=6$ but only selected ones holding measured rovibrational states beyond $P=6$. The uncertainties are given in units of 10^{-6} cm^{-1}. The values in brackets correspond to computed band origins taken from Ref. [135], their accuracy should be better than 0.1 cm^{-1}. Labels for which zero RL values are given, are printed in italics. The VBOs are ordered according to their formal labels within a given P, which corresponds to their energy order up to the reported energies and thus they appear in increasing energy order.

[b] The value of the vibrational ground state was fixed to zero with zero uncertainty.

systematic differences can be identified straightforwardly if several groups reported precise values of different accuracy for the same transitions. Inconsistencies may occur due to mistakes, but some of the inconsistencies are due to the use of different calibration standards [146–152] over time. To correct this situation properly, the best available standard frequencies must be applied to the original measured data. This process could not be followed here since the details needed are not available for the majority of the experimental studies. Nevertheless, it is straightforward to determine multiplicative recalibration factors with MARVEL [2–4].

Data from Fourier transform spectrometers are easily corrected by applying a single multiplicative recalibration factor. The procedure involves the minimization of the root-mean-square (rms) deviation between the observed transitions including the source with wavenumbers scaled with a given calibration factor and those produced by MARVEL from the energy levels. During the present MARVEL analysis of $D_2{}^{16}O$ it was found that the following sources containing FTS data require recalibration: 85CaFlMaGu [81], 89OhSa [86], 93OrRaWiWi [90], and 94ByNaSiWi [92]. The slight problem, on the order of 0.0002 cm^{-1}, with the data of 85CaFlMaGu [81] was pointed out already by Toth [91]. The rms minimization was performed sequentially for all four data sources and the recalibration factors obtained are reported in Table 4. Only the recalibrated transitions were included in the final MARVEL analysis. Recalibrated transitions are distinguished within the dataset by a letter "R" attached to the end of the transition entries.

3. MARVEL energy levels

By convention, the (0 0 0)0_{00} energy level is taken as zero with zero uncertainty. To connect the ortho and para PCs of the measured SN we used the energy difference

Table 6
MARVEL vibrational band origins (VBOs) for $D_2{}^{17}O$, with normal-mode (v_1 v_2 v_3) labels, MARVEL uncertainties (Unc.), and the number of rotational levels (RL) the vibrational bands are holding within the present database. The number of validated p-$D_2{}^{17}O$ and o-$D_2{}^{17}O$ energy levels is 189 and 149, respectively.[a]

$v_1v_2v_3$	VBO (cm^{-1})	Unc.	RL
0 0 0	0.000000[b]	0	99
0 1 0	1174.046570	2000	80
0 3 1	–		1
2 1 0	–		9
1 1 1	6512.858900	2000	96
3 0 0	–		2
2 0 1	–		51

[a] See footnote a in Table 5.
[b] See footnote b in Table 5.

Table 7
MARVEL vibrational band origins (VBOs) for $D_2{}^{18}O$, with normal-mode ($v_1v_2v_3$) labels, MARVEL uncertainties (Unc.), and the number of rotational levels (RL) the vibrational levels are holding within the present database.[a]

P	$v_1v_2v_3$	VBO (cm^{-1})	Unc.	RL
0	0 0 0	0.000000[b]	0	308
1	0 1 0	1170.157651	575	290
2	0 2 0	2320.721743	5000	211
	1 0 0	2660.793243	5000	273
	0 0 1	2767.499406	200	307
3	0 3 0	–		98
	1 1 0	–		70
	0 1 1	3927.65861	5000	125
5	1 3 0	6084.923693	707	107
	0 3 1	6191.353176	707	168
	2 1 0	6423.019593	707	158
	1 1 1	6494.740005	995	234
	0 1 2	6640.259543	1000	150
6	0 4 1	–		6
	2 2 0	–		46
	1 2 1	7626.785419	707	148
	3 0 0	–		133
	2 0 1	7859.102593	949	199
	0 2 2	–		13
	1 0 2	–		78
	0 0 3	8163.805426	1000	143
7	2 1 1	9001.453826	1000	82
	3 1 0	–		2
	1 1 2	–		1

[a] See footnote a in Table 5.
[b] See footnote b in Table 5.

between the (0 0 0)0_{00} state and the lowest para level, (0 0 0)1_{01}. This difference cannot be determined directly from experiment, but is given reliably by effective Hamiltonian fits. For $D_2{}^{16}O$, the value of 363 259.0949(7) MHz, taken from the latest version of the CDMS database [153] (version 2 from May 2011, the files are available at http://www.astro.uni-oeln.de/site/vorhersagen/catalog/archive/H2O/D2O/), was used, converted into a magic number of 12.1170191 cm^{-1}. For $D_2{}^{17}O$ and $D_2{}^{18}O$, we use values derived by Toth: 12.098600 cm^{-1} [96] and 12.082026 cm^{-1} [91], respectively. The magic number used for $D_2{}^{16}O$ was confirmed by the following analysis. The ab initio linelist of [135] was checked for near degeneracies between energy levels contained in the ortho and para PCs. Close to 700 energy level pairs, contained also in the MARVEL database, were identified which deviated from each other by less than 10^{-6} cm^{-1}. All the artificial transitions between such degenerate energy levels were added to the MARVEL input connecting the two PCs and a refinement of the magic number was performed. The refined value agrees with the magic number chosen to better than 10^{-6} cm^{-1}.

Tables 5–7 contain MARVEL vibrational band origins (VBOs) for $D_2{}^{16}O$, $D_2{}^{17}O$, and $D_2{}^{18}O$, respectively. The same tables also give the number of rovibrational energy levels validated within this work for each VBO.

Since hot water spectra have been measured for $D_2{}^{16}O$, the largest J is high, namely $J_{max}=30$ for the (0 0 0), (0 1 0), (0 2 0), (0 0 1), (0 3 0), and (1 0 0) vibrational states. Due to the large number of measured transitions, the list of VBOs whose rovibrational levels participate in measured transitions is complete for $D_2{}^{16}O$ up to $P=6$, except (0 6 0). Beyond $P=6$, there are only a few VBOs which are known experimentally. Nevertheless, rovibrational states in many of them have been observed. The highest states for which VBOs and rovibrational levels have been measured correspond to $P=11$. The number of validated *para*-$D_2{}^{16}O$ and *ortho*-$D_2{}^{16}O$ energy levels is 6608 and 5661, respectively. Note that the 101 transitions forming floating components (FCs) involve a number of energy levels which would become part of the established set of validated energy levels when new measurements become available to connect the FCs to the PCs of the measured SN of $D_2{}^{16}O$.

As in Part III, we assign a "quality grade" A^+ to a MARVEL energy level of $D_2{}^{16}O$ when it is determined by a minimum of 13 transitions from at least 5 independent experimental investigations. Energy levels involved in at least 11 transitions from 4 or more independent experimental studies are marked as A^-. Those energy levels based on at least 9 transitions from 3 independent experiments are designated as B^+, while levels with at least 7 transitions from 2 different studies are graded as B^-. All others are given a grade of C. Energy levels are considered to be not fully validated if, for example, they are based on only one source; for these the uncertainty estimates reflect the relative precisions and not the absolute accuracies. Our recommendation for transitions is that they should be graded using the designation of the lower-graded energy level. No grading of the MARVEL energy levels was attempted for $D_2{}^{17}O$ and $D_2{}^{18}O$.

For $D_2{}^{17}O$ and $D_2{}^{18}O$ there are only 2 and 14 VBOs known experimentally, respectively. The highest VBO known for $D_2{}^{18}O$ corresponds to $P=7$ but only one of the 10 possible $P=7$ VBOs is known. While it would be simple to derive rather accurate experimental VBO estimates from the obs − calc tendencies of the $K_a=0$ energy levels for several of the missing VBOs of Table 5 and some of the missing VBOs of Table 7, the TG decided not to do this in order to keep the IUPAC-recommended energy levels fully experimental.

4. Variational validation of MARVEL energy levels

MARVEL works best if a particular energy level is at the center of a sub-network of transitions forming many cycles.

There are always energy levels which are linked to the rest of the SN by a single transition; indeed, for branches [154] there may be a series of such transitions. For these levels, MARVEL cannot truly confirm the reliability of the experimental assignment and uncertainty. Nevertheless, comparison of experimental-quality MARVEL and high-accuracy first-principles variational [135] energy levels for the D_2O isotopologues allows the straightforward identification of incorrect experimental assignments. For this purpose the adiabatic empirical PES of Ref. [135] developed for $D_2{}^{16}O$ was used without modification for all three isotopologues; only the masses were changed for $D_2{}^{17}O$ and $D_2{}^{18}O$. The standard deviations, see Table 8, between the MARVEL energy levels and their variational nuclear motion counterparts, obtained with the PES reported in Ref. [135] and an exact kinetic energy operator, confirm both the high quality of the first-principles results and the correctness of the MARVEL energy levels. For $D_2{}^{17}O$, for example, the maximum deviation between the MARVEL and the first-principles computed energy levels is a mere 0.085 cm^{-1}.

For $D_2{}^{17}O$ and $D_2{}^{18}O$, fewer VBOs and lower J-value states are involved in the measured transitions. Thus, the analysis only involves levels below the barrier to linearity of water [138–140]; under these circumstances the RRD analysis of the computed rovibrational wavefunctions provide full verification of most of the labels. Above the barrier to linearity there are difficulties in many cases with assigning standard quantum numbers due to re-arrangement of the energy levels [155]. For $D_2{}^{16}O$, the great majority of the labels of the energy levels below the barrier to linearity [138–140] are confirmed, as well. Above this energy, however, the labels for higher J states have less physical significance (small RRD coefficients within the RRD tables); mixing becomes overwhelming, and no single label can be chosen.

The MARVEL energy levels of the three D_2O isotopologues were also checked against each other to ensure that their values and labels are internally consistent. After a few relabelings, no outliers were found.

Table 8
Standard deviation (SD) of the $D_2{}^{16}O$, $D_2{}^{17}O$, and $D_2{}^{18}O$ MARVEL energy levels with respect to fully converged energies obtained from variational nuclear motion computations executed with a PES reported in Ref. [135] and an exact internal-coordinate kinetic energy operator.

J	$D_2{}^{16}O$		$D_2{}^{17}O$		$D_2{}^{18}O$	
	No. of levels	SD	No. of levels	SD	No. of levels	SD
0	78	0.0234	2	0.0516	14	0.0265
1	270	0.0220	10	0.0341	55	0.0241
2	475	0.0315	19	0.0386	93	0.0237
3	673	0.0294	26	0.0390	136	0.0237
4	842	0.0334	39	0.0380	178	0.0235
5	997	0.0313	45	0.0359	212	0.0243
6	1069	0.0323	49	0.0373	246	0.0244
7	1104	0.0351	45	0.0391	285	0.0257
8	1037	0.0369	37	0.0403	288	0.0270
9	950	0.0385	29	0.0401	289	0.0294
10	851	0.0439	18	0.0356	286	0.0306
all	8346	0.0348	319	0.0381	2082	0.0263

5. Status of highly accurate transitions

In 2010 and 2013 Cazzoli, Puzzarini and co-workers [118,120] reported a few mostly unperturbed $D_2{}^{16}O$ transition frequencies in the millimeter, submillimeter, and THz regions with an unprecedented 1 kHz accuracy. Reproduction of these selected high-accuracy transitions with MARVEL energy levels is provided in Table 9.

MARVEL can reproduce these measurements extremely well, in fact even better than the stated uncertainty of the MARVEL transitions would suggest, which are themselves between 1 and 3 kHz. This is a pleasing result as the energy levels participating in the accurate transitions are involved in a large number of other transitions of much lower accuracy which could distort their prediction. This

Table 9
Reproduction of highly accurate experimental transition data, given in MHz, by MARVEL energy levels of A^+ quality for $D_2{}^{16}O$.

Transition	MARVEL	Experiment	Source
(0 0 0) 5_{23}–6_{16}	93 350.1854(25)	93 350.1855(9)	10CaDoPuGa [118]
(0 0 0) 6_{24}–7_{17}	104 875.7306(29)	104 875.7306(9)	10CaDoPuGa [118]
(0 0 0) 3_{21}–4_{14}	151 710.3774(29)	151 710.3774(7)	10CaDoPuGa [118]
(0 0 0) 5_{51}–6_{42}	180 171.1475(29)	180 171.1477(14)	10CaDoPuGa [118]
(0 0 0) 4_{22}–5_{15}	181 833.1753(29)	181 833.1754(10)	10CaDoPuGa [118]
(0 0 0) 5_{50}–6_{43}	187 633.2526(29)	187 633.2526(12)	10CaDoPuGa [118]
(0 0 0) 6_{51}–7_{44}	192 519.5038(29)	192 519.5039(15)	10CaDoPuGa [118]
(0 0 0) 1_{01}–1_{10}	316 799.8415(11)	316 799.8414(4)	10CaDoPuGa [118]
(0 0 0) 4_{31}–5_{24}	339 035.1095(25)	339 035.1096(10)	10CaDoPuGa [118]
(0 0 0) 7_{25}–8_{18}	393 332.8076(25)	393 332.8076(13)	10CaDoPuGa [118]
(0 0 0) 7_{71}–8_{62}	403 251.6307(29)	403 251.6307(20)	10CaDoPuGa [118]
(0 0 0) 7_{70}–8_{63}	403 377.3415(29)	403 377.3415(17)	10CaDoPuGa [118]
(0 0 0) 2_{02}–2_{11}	403 561.9930(29)	403 561.9929(7)	10CaDoPuGa [118]
(0 0 0) 7_{25}–7_{34}	1 043 212.702(11)	1 043 212.702(1)	13CaPu [120]
(0 0 0) 3_{13}–3_{22}	1 065 096.945(60)	1 065 096.946(30)	13CaPu [120]
(0 0 0) 8_{26}–8_{35}	1 074 239.989(11)	1 074 239.989(1)	13CaPu [120]
(0 0 0) 5_{05}–5_{14}	1 076 226.546(60)	1 076 226.546(30)	13CaPu [120]
(0 0 0) 9_{27}–9_{36}	1 194 842.468(11)	1 194 842.468(1)	13CaPu [120]

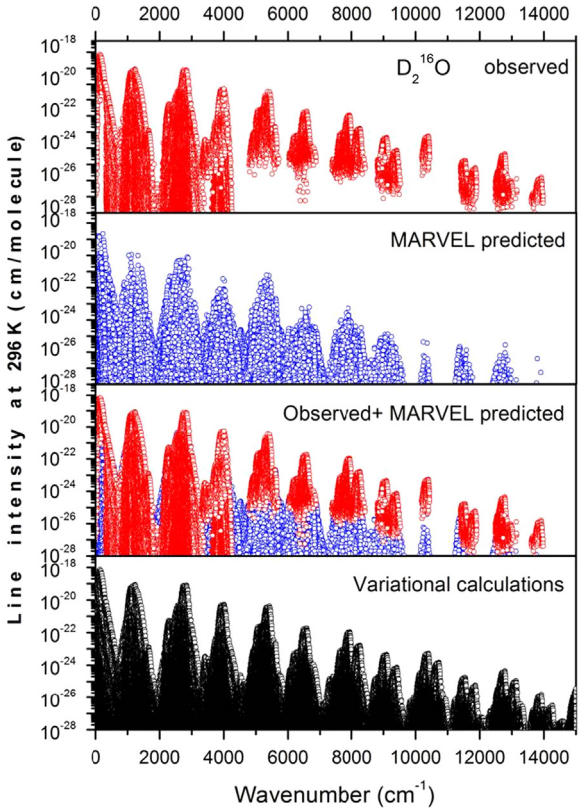

Fig. 1. Comparison of observed (top panel), MARVEL predicted (second panel, not containing any measured transitions), observed plus MARVEL predicted (third panel), and the full variational line list (bottom panel) one-photon absorption transitions for $D_2{}^{16}O$. Calculated line intensities [133] corresponding to 296 K are used in each case and only those predicted MARVEL lines are shown in the figure for which there is full agreement between the MARVEL and Ref. [133] positions and labels. Many emission measurements have been performed for $D_2{}^{16}O$, explaining the large number of very low intensity "observed" transitions on the top panel, which are yet to be measured directly in absorption.

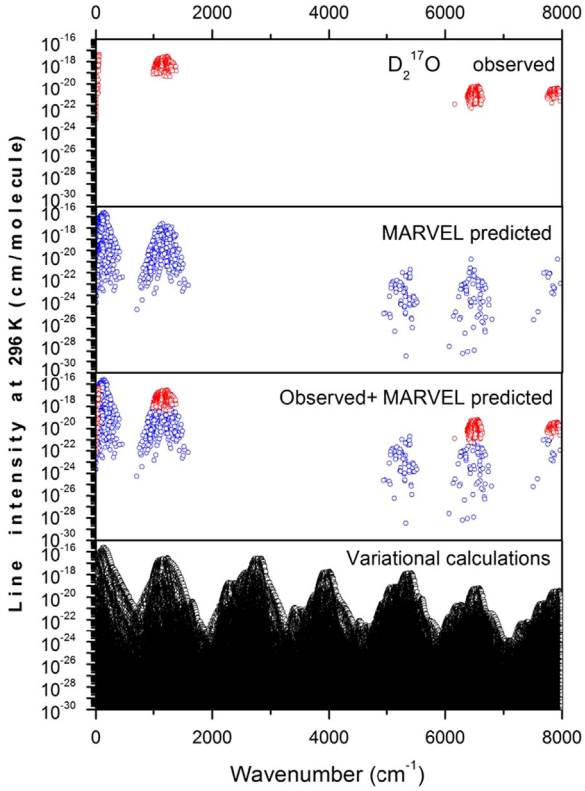

Fig. 2. Comparison of observed (top panel), MARVEL predicted (second panel, not containing any of the measured transitions), observed plus MARVEL predicted (third panel), and the full list of variational (bottom panel) one-photon absorption transitions for $D_2{}^{17}O$. Calculated line intensities [133] corresponding to 296 K are used in each case and only those predicted MARVEL lines are shown in the figure for which there is full agreement between the MARVEL and Ref. [133] positions and labels.

distortion is not reflected in the predicted frequency, just to a small extent in the uncertainties attached to the MARVEL energy levels.

6. Conclusions

Among many other applications which need high-quality molecular data, spectroscopic measurements related to different stars and the atmospheres of planets and exoplanets are of special relevance. Precise positions, intensities and line shapes are required to detect a species and quantify the amount present. Among the species for which spectroscopic data is needed for this or any other important scientific or engineering applications, water is probably the single most important one. Thus, the study of the complete spectra of water isotopologues is of prime importance. At the same time, the high-resolution rovibrational spectra of the isotopologues of the water molecule form a fertile test ground for different experimental and theoretical approaches.

The ambitious goal of our IUPAC TG has been the creation of a comprehensive database for all the important isotopologues of water. With this study the first step, determining energy levels from available measurements, is completed for the doubly deuterated water isotopologues. The present paper provides, for the first time, a dependable and carefully validated set of experimental energy levels and transition wavenumbers, all with dependable and self-consistent uncertainties, for $D_2{}^{16}O$, $D_2{}^{17}O$, and $D_2{}^{18}O$. As shown in this work, the MARVEL approach [6–9], combined with results from fourth-age [156] nuclear-motion computations, provides an ideal platform to achieve the stated goal of the TG. This statement is true not only for water isotopologues, but also for all molecules whose high-resolution spectra are studied. MARVEL has already been used for deriving experimental energy levels for the main ketene isotopologue [157] and for H_3^+ [158] and its partially deuterated isotopologues [159].

The derived MARVEL energy levels permit many inaccurate line positions predicted variationally to be replaced with MARVEL transitions characterized by low and well-defined uncertainties. The observed MARVEL and variational positions combined with predicted intensities will facilitate future high-resolution studies of these species.

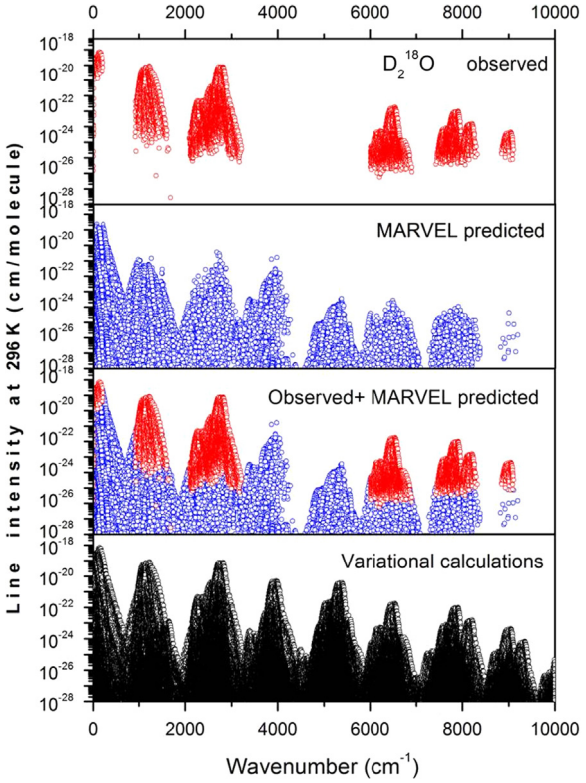

Fig. 3. Comparison of observed (top panel), MARVEL predicted (second panel, not containing any of the measured transitions), observed plus MARVEL predicted (third panel), and the full list of variational (bottom panel) one-photon absorption transitions for $D_2{}^{18}O$. Calculated line intensities [133] corresponding to 296 K are used in each case and only those predicted MARVEL lines are shown in the figure for which there is full agreement between the MARVEL and Ref. [133] positions and labels.

Observed, MARVEL predicted, and variational $D_2{}^{16}O$, $D_2{}^{17}O$, and $D_2{}^{18}O$ transitions are shown in panels of Figs. 1–3. As Fig. 1 shows, more experimental research is needed below about 320 and above 4000 cm^{-1} for $D_2{}^{16}O$ to support the remote-sensing applications mentioned in Section 1. Comparison of the first two panels of the three figures also suggests that creation and analysis of the information systems reported herein will make new analyses of new infrared spectra relatively straightforward.

The distributed information system W@DIS [160,161], one of the intended end products of the effort of this IUPAC TG, contains the levels and lines validated in this study for the three D_2O isotopologues. It can be accessed via http://wadis.saga.iao.ru. The official MARVEL site, http://kkrk.chem.elte.hu/marvel, also lists the IUPAC lines and levels and will be the home of future updates.

Table 10 summarizes the results of the activities of the TG by providing the number of rovibrational transitions analyzed and validated and the number of validated MARVEL energy levels for nine water isotopologues. As expected, it is $H_2{}^{16}O$ for which the largest amount of validated transitions and energy levels exist, followed by $HD^{16}O$ and $D_2{}^{16}O$. Experimental data on the rovibrational energy level structure of isotopologues containing ^{17}O remains scarce. It is hoped that the ready availability of experimental-quality labeled energy levels will lead to the analysis of many new spectra eventually yielding the missing information. Finally we note that as a follow-on activity from the work of the TG reported here, the representation of line profiles for water transitions has been considered and recommendations were made for moving beyond Voigt profiles [162] by another IUPAC TG formed with the participation of several authors of this study.

Table 10
Summary of IUPAC TG results for measured transitions analyzed and energy levels determined for different isotopologues of the water molecule.

Species	Transitions		Energy levels			Ref.
	Identified	Validated[a]	Ortho	Para	Sum	
$H_2{}^{16}O$	184 667	182 156	10 446	8040	18 486	[4]
$H_2{}^{18}O$	32 325	31 705	2801	2330	5131	[2,3]
$H_2{}^{17}O$	9169	9028	1547	1176	2723	[2,3]
$HD^{16}O$	54 740	53 291			8818	[3]
$HD^{18}O$	8729	8634			1864	[3]
$HD^{17}O$	485	478			162	[3]
$D_2{}^{16}O$	53 534	52 842	5661	6608	12 269	This work
$D_2{}^{18}O$	12 167	12 026	1506	1845	3351	This work
$D_2{}^{17}O$	600	583	165	173	338	This work

[a] Although transitions within a floating component of a spectroscopic network [39,40] can be perfectly valid, they cannot be validated via the MARVEL protocol utilized by the TG, contributing to the number of unvalidated transitions. Newly measured transitions are required to connect these floating components to the rooted principal components of the SN, thus allowing the straightforward validation of these previously measured transitions.

Acknowledgments

We all thank the International Union of Pure and Applied Chemistry for funding under project 2004-035-1-100 (A database of water transitions from experiment and theory). In addition, this work has received partial support from the UK Natural Environment Research Council, ERC Advanced Investigator Project 267219, the Royal Society, the Scientific Research Fund of Hungary (Grant OTKA NK83583), the Russian Foundation for Basic Research, the Belgian Federal Science Policy Office (contracts EV/35/3A, SD/AT/01A, PRODEX 1514901NLSFe(IC)), the Belgian National Fund for Scientific Research (FRFC contracts), the Communauté de Belgique (Action de Recherche Concertées), the COST Action CoDECS (CM1002), and the NASA AURA mission, under the grant NNX11AF91G. Part of the research described in this paper was performed at the Jet Propulsion Laboratory, California Institute of Technology, under contracts and grants with NASA. Alain Campargue and Ludovic Daumont are grateful for the financial support provided by the Programme National LEFE (CHAT) of CNRS (INSU). Semen Mikhailenko is thanked for providing part of the $D_2{}^{16}O$ dataset used during this study. We thank Christina Puzzarini for help deperturbing the published frequencies given in 13CaPu.

Appendix A. Supplementary data

Supplementary data associated with this article can be found in the online version at http://dx.doi.org/10.1016/j.jqsrt.2014.03.019.

References

[1] Tennyson J, Bernath PF, Brown LR, Campargue A, Császár AG, Daumont L, et al. A database of water transitions from experiment and theory (IUPAC technical report). Pure Appl Chem 2014;86:71–83.

[2] Tennyson J, Bernath PF, Brown LR, Campargue A, Carleer MR, Császár AG, et al. IUPAC critical evaluation of the rotational–vibrational spectra of water vapor. Part I. Energy levels and transition wavenumbers for $H_2{}^{17}O$ and $H_2{}^{18}O$. J Quant Spectrosc Radiat Transfer 2009;110:573–96.

[3] Tennyson J, Bernath PF, Brown LR, Campargue A, Carleer MR, Császár AG, et al. IUPAC critical evaluation of the rotational–vibrational spectra of water vapor. Part II. Energy levels and transition wavenumbers for $HD^{16}O$, $HD^{17}O$, and $HD^{18}O$. J Quant Spectrosc Radiat Transfer 2010;110:2160–84.

[4] Tennyson J, Bernath PF, Brown LR, Campargue A, Császár AG, Daumont L, et al. IUPAC critical evaluation of the rotational–vibrational spectra of water vapor. Part III. Energy levels and transition wavenumbers for $H_2{}^{16}O$. J Quant Spectrosc Radiat Transfer 2013;117:29–58.

[5] Bernath PF. The spectroscopy of water vapour: experiment, theory and applications. Phys Chem Chem Phys 2002;4:1501–9.

[6] Császár AG, Czakó G, Furtenbacher T, Mátyus E. An active database approach to complete spectra of small molecules. Ann Rep Comput Chem 2007;3:155–76.

[7] Furtenbacher T, Császár AG, Tennyson J. MARVEL: measured active rotational–vibrational energy levels. J Mol Spectrosc 2007;245:115–25.

[8] Furtenbacher T, Császár AG. On employing $H_2{}^{16}O$, $H_2{}^{17}O$, $H_2{}^{18}O$, and $D_2{}^{16}O$ lines as frequency standards in the 15–170 cm^{-1} window. J Quant Spectrosc Radiat Transfer 2008;109:1234–51.

[9] Furtenbacher T, Császár AG. MARVEL: measured active rotational–vibrational energy levels. II. Algorithmic improvements. J Quant Spectrosc Radiat Transfer 2012;113:929–35.

[10] Rothman LS, Gordon IE, Babikov Y, Barbe A, Benner DC, Bernath PF, et al. The *HITRAN*2012 molecular spectroscopic database. J Quant Spectrosc Radiat Transfer 2013;130:4–50.

[11] Jacquinet-Husson N, Crepeau L, Armante R, Boutammine C, Chédin A, Scott NA, et al. The 2009 edition of the GEISA spectroscopic database. J Quant Spectrosc Radiat Transfer 2011;112:2395–445.

[12] Kirschenbaum I. Physical properties and analysis of heavy water. New York: Mc-Graw Hill; 1951.

[13] Keenand JH, Keyes FG, Hill PG, Moore JG. Steam tables. New York: John Wiley and Sons Inc.; 1969.

[14] Hill PG, MacMillan R, Lee V. A fundamental equation of state for heavy water. J Phys Chem Ref Data 1982;11:1–14.

[15] Kostrowicka Wyczalkowska A, Abdulkadirova KS, Anisimov MA, Sengers JV. Thermodynamic properties of H_2O and D_2O in the critical region. J Chem Phys 2000;11:4985–5002.

[16] Wagner W, Pruss A. The IAPWS formulation 1995 for the thermodynamic properties of ordinary water substance for general and scientific use. J Phys Chem Ref Data 2002;31:387–535.

[17] Revised release on the IAPS formulation 1984 for the thermodynamic properties of heavy water substance. URL: ⟨http://www.iapws.org⟩.

[18] Nabiev SS, Vaks VL, Domracheva EG, Palkina LA, Pripolzin SI, Sobakinskaya EA, et al. Express analysis of water isotopomers in the atmosphere with the use of nonstationary subterahertz and terahertz spectroscopy methods. Atmos Ocean Opt 2011;24:402–10.

[19] DeBerg C, Bézard B, Owen T, Crisp D, Maillard J-P, Lutz BL. Deuterium on Venus—observations from Earth. Science 1991;251:547–9.

[20] Krasnopolsky VA, Belyaev DA, Gordon IE, Li G, Rothman LS. Observations of D/H ratios in H_2O, HCl, and HF on Venus and new DCl and DF line strengths. Icarus 2013;224:57–65.

[21] Herbst E. Isotopic fractionation by ion-molecule reactions. Space Sci Rev 2003;106:293–304.

[22] Coutens A, Vastel C, Cazaux S, Bottinelli S, Caux E, Ceccarelli C, et al. Heavy water stratification in a low-mass protostar. Astron Astrophys 2013;553:A75.

[23] Roueff E, Tiné S, Coudert LH, Pineau des Forets G, Falgarone E, Gerin M. Detection of doubly deuterated ammonia in L134N. Astron Astrophys 2000;354:L63–6.

[24] Lis D, Roueff E, Gerin M, Phillips TG, Coudert, van der Tak FFS, et al. Detection of triply deuterated ammonia in the Barnard 1 cloud. Astrophys J 2002;571:L55–8.

[25] van der Tak FFS, Schilke P, Müller HSP, Lis DC, Phillips TG. Triply deuterated ammonia in NGC 1333. Astron Astrophys 2002;388:L53–6.

[26] Vastel C, Phillips TG, Yoshida H. Detection of D_2H^+ in the dense interstellar medium. Astrophys J Lett 2004;606:L127.

[27] Vastel C, Phillips TG, Ceccarelli C, Pearson J. First detection of doubly deuterated hydrogen sulfide. Astrophys J 2003;593:L97–100.

[28] Turner BE. Detection of doubly deuterated interstellar formaldehyde (D_2CO)—an indicator of active grain surface chemistry. Astrophys J Lett 1990;347:L29–33.

[29] Marcelino N, Cernicharo J, Roueff E, Gerin M, Mauersberger R. Deuterated thioformaldehyde in the Barnard 1 cloud. Astrophys J 2005;620:308.

[30] Spezzano S, Brunken S, Schilke P, Caselli P, Menten KM, McCarthy MC, et al. Interstellar detection of $c\text{-}C_3D_2$. Astrophys J Lett 2013;769:L19.

[31] Butner HM, Charnley SB, Ceccarelli C, Rodgers SD, Pardo JR, Parise B, et al. Discovery of interstellar heavy water. Astrophys J 2007;659:L137.

[32] Vastel C, Ceccarelli C, Caux E, Coutens A, Cernicharo J, Bottinelli S, et al. Ortho-to-para ratio of interstellar heavy water. Astron Astrophys 2010;521:L31.

[33] Neill JL, Crockett NR, Bergin EA, Pearson JC, Xu L-H. Deuterated molecules in Orion KL from Herschel/HIFI. Astrophys J 2013;777:85. http://dx.doi.org/10.1088/0004-637X/777/2/85.

[34] Braly LB, Cruzan JD, Liu K, Fellers RS, Saykally RJ. Terahertz laser spectroscopy of the water dimer intermolecular vibrations. I. $(D_2O)_2$. J Chem Phys 2000;112:10293–313.

[35] Buhr H, Stuetzel J, Mendes MB, Novotny O, Schwalm D, Berg MH, et al. Hot water molecules from dissociative recombination of D_3O^+ with cold electrons. Phys Rev Lett 2010;105:103202.

[36] Barber RJ, Miller S, Dello Russo N, Mumma MJ, Tennyson J, Guio P. Water in the near IR spectrum of comet 8P/Tuttle. Mon Not R Astron Soc 2009;398:1593–600.

[37] Michael EA, Keoshian CJ, Wagner DR, Anderson SK, Saykally RJ. Infrared water recombination lasers. Chem Phys Lett 2001;338:277–84.

[38] Michael EA, Keoshian CJ, Anderson SK, Saykally RJ. Rotational transitions in excited vibrational states of D_2O. J Mol Spectrosc 2001;208:219–23.

[39] Császár AG, Furtenbacher T. Spectroscopic networks. J Mol Spectrosc 2011;266:99–103.

[40] Furtenbacher T, Császár AG. The role of intensities in determining characteristics of spectroscopic networks. J Mol Struct 2012;108:123–9.

[41] Furtenbacher T, Arenda´s P, Mellau, G, Csa´sza´r AG. Simplemolecules as complex systems. Sci. Rep. 2014;4;4654. http://dx.doi.org/10.1038/srep04654.

[42] Watson JKG. Robust weighting in least-squares fits. J Mol Spectrosc 2003;219:326–8.

[43] Miani A, Tennyson J. Can ortho–para transitions for water be observed? J Chem Phys 2004;120:2732–9.

[44] Ellis JW, Sorge BW. The infrared absorption spectrum of water containing deuterium. J Chem Phys 1934;2:559–64.

[45] Rank DH, Larsen KD, Bordner ER. The Raman spectrum of heavy water vapor. J Chem Phys 1934;2:464–7.

[46] Wood RW. Raman spectrum of heavy-water vapour. Phys Rev 1934;45:732–3.

[47] Barker EF, Sleator WW. The infrared spectrum of heavy water. J Chem Phys 1935;3:660–3.

[48] Norris WV, Unger HJ, Holmquist RE. An infrared absorption band of heavy water vapor. Phys Rev 1936;49:272.

[49] Fuson N, Randall HM, Dennison DM. The far infra-red absorption spectrum and the rotational structure of the heavy water vapor molecule. Phys Rev 1939;56:982–1000.

[50] King GW. The asymmetric rotor. IV. An analysis of the 8.5−μ band of D_2O by punched-card techniques. J Chem Phys 1947;15:85–8.

[51] Dickey FP, Nielsen HH. The infra-red spectrum of heavy water vapor. Phys Rev 1948;73:1164–73.

[52] Ginsburg N. Additional rotational energy levels of H_2O and D_2O molecules. Phys Rev 1948;74:1052–7.
[53] Strandberg MWP. Microwave rotational absorption in D_2O. Phys Rev 1948;74:1245.
[54] Innes KK, Cross PC, Giguère PA. The asymmetric rotor IX The heavy water bands at 2787 cm^{-1} and 5373 cm^{-1}. J Chem Phys 1951;19: 1086–8.
[55] Beard CI, Bianco DR. Two D_2O microwave absorption lines. J Chem Phys 1952;20:1488–9.
[56] Dickey FP, Guderjahn CA, Palik ED. The combination band $\nu_1+\nu_2+\nu_3$ of heavy water vapor. J Chem Phys 1952;20:375–7.
[57] Benedict WS, Gailar N, Plyler EK. The vibration–rotation spectrum of D_2O. J Chem Phys 1953;21:1301–2.
[58] Crawford HD. Two new lines in the microwave spectrum of heavy water. J Chem Phys 1953;21:2099.
[59] Jen CK, Bianco DR, Massey JT. Some heavy water rotational absorption lines. J Chem Phys 1953;21:520–5.
[60] Posener DW, Strandberg MWP. Centrifugal distortion effect in asymmetric top molecules. III. H_2O, D_2O, and HDO. Phys Rev 1954;95:374–84.
[61] Dickey FP, Hoffman JM. Vibration–rotation band ν_2 of heavy water vapor. J Chem Phys 1955;23:1718–20.
[62] Benedict WS, Gailar N, Plyler EK. Rotation–vibration spectra of deuterated water vapor. J Chem Phys 1956;24:1139–65.
[63] Erlandsson G, Cox J. Millimeter-wave lines of heavy water. J Chem Phys 1956;25:778–9.
[64] Verhoeven J, Bluyssen H, Dymanus A. Hyperfine structure of HDO and D_2O by beam maser spectroscopy. Phys Lett A 1967;25:214–5.
[65] Harvey KB, Shurvell HF. Infrared absorption of D_2O in solid nitrogen. J Mol Spectrosc 1968;25:120–2.
[66] Verhoeven J, Bluyssen H, Dymanus A. Hyperfine structure of HDO and D_2O by beam maser spectroscopy. Phys Lett A 1968;26:424–5.
[67] Benedict WS, Clough SA, Frenkel L, Sullivan TE. Microwave spectrum and rotational constants for the ground state of D_2O. J Chem Phys 1970;53:2565–70.
[68] Bellet J, Steenbeckeliers G. Calcul des constantes rotationnelles des molecules H_2O, HDO et D_2O dans leurs etats fondamentaux de vibration. C R Acad Sci B 1970;271:1208–11.
[69] Steenbeckeliers G, Bellet J. Spectre de rotation de l'eau lourde. C R Acad Sci B 1970;270:1039–41.
[70] Stephenson DA, Strauch RG. Water vapor spectrum near 600 GHz. J Mol Spectrosc 1970;35:494–5.
[71] Verhoeven J, Dymanus A. Magnetic properties and molecular quadrupole tensor of the water molecule by beam-maser Zeeman spectroscopy. J Chem Phys 1970;52:3222–33.
[72] Lin CL, Shaw JH. Measurement and analysis of the ν_2 band of $D_2{}^{16}O$. J Mol Spectrosc 1977;66:441–7.
[73] Steenbeckeliers G, Bellet J. Application of Watson's centrifugal distortion theory to water and light asymmetric tops. General methods. Analysis of the ground state and the ν_2 state of $D_2{}^{16}O$. J Mol Spectrosc 1973;45:10–34.
[74] Fleming JW, Gibson MJ. Far-infrared absorption spectra of water vapor $H_2{}^{16}O$ and isotopic modifications. J Mol Spectrosc 1976;62: 326–37.
[75] Lovas FJ. Microwave spectral tables. II. Triatomic molecules. J Phys Chem Ref Data 1978;7:1445–750.
[76] Dodel G, Douglas NG. Separation of the $5_5-5_3/5_4-5_2$ doublet in the ν_2 band of D_2O. J Mol Spectrosc 1981;87:297.
[77] Papineau N, Flaud J-M, Camy-Peyret C, Guelachvili G. The $2\nu_2$, ν_1 and ν_3 bands of $D_2{}^{16}O$. The ground state (000) and the triad of interacting states (020), (100), (001). J Mol Spectrosc 1981;87:219–32.
[78] Bykov AD, Lopasov VP, Makushkin YS, Sinitsa LN, Ulenikov ON, Zuev VE. Rotation–vibration spectra of deuterated water vapor in the 9160–9390 cm^{-1} region. J Mol Spectrosc 1982;94:1–27.
[79] De Temple TA. List of the optically pumped laser lines of D_2O. Rev Infrared Millim Waves 1984;2:337.
[80] Messer JK, DeLucia FC, Helminger P. Submillimeter spectroscopy of the major isotopes of water. J Mol Spectrosc 1984;105:139–55.
[81] Camy-Peyret C, Flaud J-M, Mahmoudi A, Guelachvili G, Johns JWC. Line positions and intensities in the ν_2 band of D_2O improved pumped D_2O laser frequencies. Int J Infrared Millim Waves 1985;6: 199–233.
[82] Johns JWC. High-resolution far-infrared (20–350-cm^{-1}) spectra of several isotopic species of H_2O. J Opt Soc Am B 1985;2: 1340–54.
[83] Thakur KB, Rinsland CP, Smith MAH, Benner DC, Devi VM. Absolute line intensity measurements in the ν_2 bands of HDO and D_2O using a tunable diode laser spectrometer. J Mol Spectrosc 1986;120: 239–45.
[84] Baskakov OI, Alekseev VA, Alekseev EA, Polevoi BI. New submillimeter lines of water and its isotopes. Opt Spektrosk 1987;63: 1016–8.
[85] Bykov AD, Makarov VS, Moskalenko NI, Naumenko OV, Ulenikov ON, Zotov OV. Analysis of the D_2O absorption spectrum near 2.5 μm. J Mol Spectrosc 1987;123:126–34.
[86] Ohshima T, Sasada H. 1.5−μm DFB semiconductor laser spectroscopy of deuterated water. J Mol Spectrosc 1989;136:250–63.
[87] Rinsland CP, Smith MAH, Devi VM, Benner DC. Measurements of Lorentz-broadening coefficients and pressure-induced line-shift coefficients in the ν_2 band of of $D_2{}^{16}O$. J Mol Spectrosc 1991;150: 173–83.
[88] Sasada H, Takeuchi S, Iritani M, Nakatani K. Semiconductor-laser heterodyne frequency measurements of 1.52 μm molecular transitions. J Opt Soc Am B 1991;8:713–8.
[89] Rinsland CP, Smith MAH, Devi VM, Benner DC. Measurements of Lorentz-broadening coefficients and pressure-induced line-shift coefficients in the ν_1 band of $HD^{16}O$ and the ν_3 band of $D_2{}^{16}O$. J Mol Spectrosc 1992;156:507–11.
[90] Ormsby PS, Rao KN, Winnewisser M, Winnewisser BP, Naumenko OV, Bykov AD, et al. The $3\nu_2+\nu_3, \nu_1+\nu_2+\nu_3, \nu_1+3\nu_2, 2\nu_1+\nu_2$, and $\nu_2+2\nu_3$ bands of $D_2{}^{16}O$: the second hexade of interacting states. J Mol Spectrosc 1993;158:109–30.
[91] Toth RA. $D_2{}^{16}O$ and $D_2{}^{18}O$ transition frequencies and strengths in the ν_2 bands. J Mol Spectrosc 1993;162:41–54.
[92] Bykov AD, Naumenko OV, Sinitsa LN, Winnewisser BP, Winnewisser M, Ormsby PS, et al. The hot band $\nu_1+2\nu_2+\nu_3-\nu_2$ of $D_2{}^{16}O$. J Mol Spectrosc 1994;166:169–75.
[93] Paso R, Horneman V-M. High-resolution rotational absorption spectra of $H_2{}^{16}O$, $HD^{16}O$, and $D_2{}^{16}O$ between 110 and 500 cm^{-1}. J Opt Soc Am B 1995;12:1813–38.
[94] Cohen Y, Bar I, Rosenwaks S. Spectroscopy of D_2O (2,0,1). J Mol Spectrosc 1996;180:298–304.
[95] Toth RA. HDO and D_2O low pressure, long path spectra in the 600–3100 cm^{-1} region. I. HDO line positions and strengths. J Mol Spectrosc 1999;195:73–97.
[96] Toth RA. HDO and D_2O low pressure, long path spectra in the 600–3100 cm^{-1} region. II. D_2O line positions and strengths. J Mol Spectrosc 1999;195:98–122.
[97] Bykov A, Naumenko O, Sinitsa L, Voronin B, Winnewisser BP. The $3\nu_2$ band of $D_2{}^{16}O$. J Mol Spectrosc 2000;199:158–65.
[98] He S-G, Ulenikov ON, Onopenko GA, Bekhtereva ES, Wang X-H, Hu S-M, et al. High-resolution Fourier transform spectrum of the D_2O molecule in the region of the second triad of interacting vibrational states. J Mol Spectrosc 2000;200:34–9.
[99] Ulenikov ON, He S-G, Onopenko GA, Bekhtereva ES, Wang X-H, Hu S-M, et al. High-resolution study of the $(\nu_1+1/2\nu_2+\nu_3=3)$ polyad of strongly interacting vibrational bands of D_2O. J Mol Spectrosc 2000;204:216–25.
[100] Wang X, Ulenikov ON, Onopenko GA, Bekhtereva ES, He S-G, Hu S-M, et al. High-resolution study of the first hexad of D_2O. J Mol Spectrosc 2000;200:25–33.
[101] Matsushima F, Matsunaga M, Qian G-Y, Ohtaki Y, Wang R-L, Takagi K. Frequency measurement of pure rotational transitions of D_2O from 0.5 to 5 THz. J Mol Spectrosc 2001;206:41–6.
[102] Ulenikov ON, Hu S-M, Bekhtereva ES, Onopenko GA, He S-G, Wang X-H, et al. High-resolution Fourier transform spectrum of D_2O in the region near 0.97 μm. J Mol Spectrosc 2001;210:18–27.
[103] Zheng JJ, Ulenikov ON, Onopenko GA, Bekhtereva ES, He SG, Wang XH, et al. High-resolution vibration–rotation spectrum of D_2O in the region near the $2\nu_1+\nu_2+\nu_3$ absorption band. Mol Phys 2001;99:931–7.
[104] Hu S-M, Ulenikov ON, Bekhtereva ES, Onopenko GA, He S-G, Lin H, et al. High-resolution Fourier-transform intracavity laser absorption spectroscopy of D_2O in the region of the $4\nu_1+\nu_3$ band. J Mol Spectrosc 2002;212:89–95.
[105] Mellau G, Mikhailenko SN, Starikova EN, Tashkun SA, Over H, Tyuterev VG. Rotational levels of the (000) and (010) states of $D_2{}^{16}O$ from hot emission spectra in the 320–860 cm^{-1} region. J Mol Spectrosc 2004;224:32–60.
[106] Shirin SV, Zobov NF, Polyansky OL, Tennyson J, Parekunnel T, Bernath PF. Analysis of hot D_2O emission using spectroscopically determined potentials. J Chem Phys 2004;120:206–10.
[107] Mikhailenko SN, Mellau GC, Starikova EN, Tashkun SA, Tyuterev VG. Analysis of the first triad of interacting states (020), (100), and (001) of $D_2{}^{16}O$ from hot emission spectra. J Mol Spectrosc 2005;233:32–59.
[108] Naumenko OV, Leshchishina O, Shirin S, Jenouvrier A, Fally S, Vandaele AC, et al. Combined analysis of the high sensitivity

Fourier transform and ICLAS-VeCSEL absorption spectra of D_2O between 8800 and 9520 cm^{-1}. J Mol Spectrosc 2006;238:79–90.
[109] Yu BL, Yang Y, Zeng F, Alfano RR. Terahertz absorption spectrum of D_2O vapour. Opt Commun 2006;258:256–63.
[110] Zobov NF, Ovsannikov RI, Shirin SV, Polyansky OL, Tennyson J, Janka A, et al. Infrared emission spectrum of hot D_2O. J Mol Spectrosc 2006;240:112–9.
[111] Brünken S, Müller HSP, Endres C, Lewen F, Giesen T, Drouin B, et al. High resolution rotational spectroscopy on D_2O up to 2.7 THz in its ground and first excited vibrational bending states. Phys Chem Chem Phys 2007;9:2103–12.
[112] Campargue A, Mazzotti F, Baguier S, Polyansky OL, Vasilenko IA, Naumenko OV. High sensitivity ICLAS of D_2O between 12450 and 12850 cm^{-1}. J Mol Spectrosc 2007;245:89–99.
[113] Naumenko OV, Mazzotti F, Leshchishina OM, Tennyson J, Campargue A. Intracavity laser absorption spectroscopy of D_2O between 11400 and 11900 cm^{-1}. J Mol Spectrosc 2007;242:1–9.
[114] Naumenko OV, Leshchishina OM, Baguier S, Campargue A. Intracavity laser absorption spectroscopy of D_2O between 12 850 and 13 380 cm^{-1}. J Mol Spectrosc 2008;252:52–9.
[115] Campargue A, Leshchishina OM, Naumenko OV. $D_2{}^{16}O$: ICLAS between 13 600 and 14 020 cm^{-1} and normal mode labeling of the vibrational states. J Mol Spectrosc 2009;254:1–9.
[116] Tashkun SA, Putilova TA. Rotational structure of the 000, 010, 100, 020, and 001 vibrational states of the $D_2{}^{16}O$ molecule: spectroscopic assignment of rotational levels up to J, $K_a=30$ and analysis of published data. Opt Spectrosc 2009;107:686–95.
[117] Bykov AD, Naumenko OV, Polovtseva ER, Hu S-M, Liu A-W. Fourier transform absorption spectrum of $D_2{}^{16}O$ in the 7360–8440 cm^{-1} spectral region. J Quant Spectrosc Radiat Transfer 2010;111:2197–210.
[118] Cazzoli G, Dore L, Puzzarini C, Gauss J. The hyperfine structure in the rotational spectra of D_2O: Lamb-dip measurements and quantum-chemical calculations. Mol Phys 2010;108:2335–42.
[119] Mikhailenko SN, Naumenko OV, Nikitin AV, Vasilenko IA, Liu A-W, Song K-F, et al. Absorption spectrum of deuterated water vapor enriched by ^{18}O between 6000 and 9200 cm^{-1}. J Quant Spectrosc Radiat Transfer 2012;113:653–69.
[120] Cazzoli G, Puzzarini C. Sub-Doppler resolution in the THz frequency domain: 1 kHz accuracy at 1 THz by exploiting the Lamb-dip technique. J Phys Chem A 2013;117:13759–66.
[121] Liu A-W, Naumenko OV, Kassi S, Campargue A. CW-cavity ring down spectroscopy of deuterated water in the 1.58 μm atmospheric transparency window. J Quant Spectrosc Radiat Transfer 2014;138:97–106.
[122] Puzzarini C, Cazzoli G, Gauss J. The rotational spectra of $HD^{17}O$ and $D_2{}^{17}O$: experiment and quantum-chemical calculations. J Chem Phys 2012;137:154311.
[123] Bellet J, Lafferty WJ, Steenbeckeliers G. Microwave spectra of $D_2{}^{17}O$ and $D_2{}^{18}O$. J Mol Spectrosc 1973;47:388–402.
[124] Di Lonardo G, Fusina L. The ν_2 band of $D_2{}^{18}O$. J Mol Spectrosc 1989;135:250–8.
[125] Wang WF, Tan TL, Tan BL, Ong PP. The ν_2 bands of $HD^{18}O$ and $D_2{}^{18}O$: rovibrational constants and additional transitions. J Mol Spectrosc 1996;176:226–8.
[126] Liu A-W, Song K-F, Ni H-Y, Hu S-M, Naumenko OV, Vasilenko IA, et al. (0 0 0) and (0 1 0) energy levels of the $HD^{18}O$ and $D_2{}^{18}O$ molecules from analysis of their ν_2 bands. J Mol Spectrosc 2011;265:26–38.
[127] Ni H-Y, Liu A-W, Song K-F, Hu S-M, Naumenko O, Kruglova T, et al. High-resolution spectroscopy of the triple-substituted isotopologue of water molecule $D_2{}^{18}O$: the first triad. Mol Phys 2008;106:1793.
[128] Toth R. Measurements of line positions and strengths of $HD^{18}O$ and $D_2{}^{18}O$ in the 2500–4280 cm^{-1} region. J Mol Struct 2005;742:49–68.
[129] Mikhailenko SN, Tashkun SA, Daumont L, Jenouvrier A, Carleer M, Fally S, et al. Line positions and energy levels of the ^{18}O substitutions from the $HDO/D_2{}^{18}O$ spectra between 5600 and 8800 cm^{-1}. J Quant Spectrosc Radiat Transfer 2010;111:2185–96.
[130] Down MJ, Tennyson J, Orphal J, Chelin P, Ruth AA. Analysis of an ^{18}O and D enhanced water spectrum and new assignments for $HD^{18}O$, $D_2{}^{18}O$ in the near-infrared region (6000–7000 cm^{-1}) using newly calculated variational line lists. J Mol Spectrosc 2012;282:1–8.
[131] King GW. Anharmonicity constants of the potential function of the water molecule. J Chem Phys 1937;5:413–5.
[132] Partridge H, Schwenke DW. The determination of an accurate isotope dependent potential energy surface for water from extensive ab initio calculations and experimental data. J Chem Phys 1997;106:4618–39.
[133] Schwenke DW, Partridge H. Convergence testing of the analytic representation of an *ab initio* dipole moment function for water: improved fitting yields improved intensities. J Chem Phys 2000;113:6592–7.
[134] Aida M, Dupuis M. IR and Raman intensities in vibrational spectra from direct ab initio molecular dynamics: D_2O as an illustration. J Mol Struct (THEOCHEM) 2003;633:247–55.
[135] Shirin SV, Zobov NF, Polyansky OL. Theoretical line list of $D_2{}^{16}O$ up to 16 000 cm^{-1} with an accuracy close to experimental accuracy. J Quant Spectrosc Radiat Transfer 2008;109:549–58.
[136] Mátyus E, Fábri C, Szidarovszky T, Czakó G, Allen W, Császár AG. Assigning quantum labels to variationally computed rotational–vibrational eigenstates of polyatomic molecules. J Chem Phys 2010;133:034113.
[137] Szidarovszky T, Fábri C, Császár AG. The role of axis embedding on rigid rotor decomposition analysis of variational rovibrational wave functions. J Chem Phys 2012;136:174112.
[138] Barletta P, Shirin SV, Zobov NF, Polyansky OL, Tennyson J, Valeev EF, et al. CVRQD adiabatic *ab initio* ground-state potential surfaces for the water molecule. J Chem Phys 2006;125:204307.
[139] Tarczay G, Császár AG, Klopper W, Szalay V, Allen WD, Schaefer III HF. The barrier to linearity of water. J Chem Phys 1999;110:11971–81.
[140] Valeev EF, Allen WD, Schaefer III HF, Császár AG. The second-order Møller–Plesset barrier to linearity of water. J Chem Phys 2001;114:2875–8.
[141] Jennings DA, Evenson KM, Di Lonardo G, Hinz A, Nolt I, Zink L. Personal communication quoted by Johns [Johns JWC. High-resolution far-infrared (20–350-cm^{-1}) spectra of several isotopic species of H_2O. J Opt Soc Am B 1985;2:1340–54.
[142] Helminger P, Messer JK, De Lucia FC. Continuously tunable coherent spectroscopy for the 0.1–1.0 THz region. Appl Phys Lett 1983;42:309–10.
[143] De Lucia FC, Helminger P, Gordy W. Submillimeter-wave spectra and equilibrium structures of hydrogen halides. Phys Rev A 1971;3:1849–57.
[144] Toth RA. $HD^{16}O$, $HD^{18}O$, and $HD^{17}O$ transition frequencies and strengths in the ν_2 bands. J Mol Spectrosc 1993;162:20–40.
[145] Orphal J, Ruth AA. High-resolution Fourier-transform cavity-enhanced absorption spectroscopy in the near-infrared using an incoherent broad-band light source. Opt Express 2008;16:19232–43.
[146] Brown LR, Toth RA. Comparison of the frequencies of NH_3, CO_2, H_2O, N_2O, CO, and CH_4 as infrared calibration standards. J Opt Soc Am B 1985;2:842–56.
[147] Maki AG, Wells JS. New wave-number calibration tables from heterodyne frequency measurements. J Res Natl Inst Stand Technol 1992;97:409–70.
[148] Guelachvili G, Birk M, Bordé CJ, Brault JW, Brown LR, Carli B, et al. High resolution wavenumber standards for the infrared. J Mol Spectrosc 1996;177:164–79.
[149] Horneman VM. High accurate peak positions for calibration purposes with the lowest fundamental bands ν_2 of N_2O and CO_2. J Mol Spectrosc 2007;241:45–50.
[150] Okubo S, Nakayama H, Iwakuni K, Inaba H, Sasada H. Absolute frequency list of the ν_3-band transitions of methane at a relative uncertainty level of 10^{-11}. Opt Express 2011;19:23878–88.
[151] Falke S, Tiemann E, Lisdat C, Schnatz H, Grosche G. Transition frequencies of the D lines of 39 K, 40 K, and 41 K measured with a femtosecond laser frequency comb. Phys Rev A 2006;74:032503.
[152] Liao CC, Wu KY, Lien YH, Knoeckel H, Chui HC, Tiemann E, et al. Precise frequency measurements of $^{127}I_2$ lines in the wavelength region 750–780 nm. J Opt Soc Am B—Opt Phys; 2010;27:1208–14, http://dx.doi.org/10.1364/JOSAB.27.001208.
[153] Müller HSP, Schlöder F, Stutzki J, Winnewisser G. The Cologne database for molecular spectroscopy, CDMS: a useful tool for astronomers and spectroscopists. J Mol Struct 2005;742:215–27.
[154] Polyansky OL, Zobov NF, Viti S, Tennyson J, Bernath PF, Wallace L. K band spectrum of water in sunspots. Astrophys J 1997;489:L205–8.
[155] Child MS, Weston T, Tennyson J. Quantum monodromy in the spectrum of H_2O and other systems: new insight into the level structures of quasi-linear molecules. Mol Phys 1999;96:371–9.
[156] Császár AG, Fábri C, Szidarovszky T, Mátyus E, Furtenbacher T, Czakó G. Fourth age of quantum chemistry: molecules in motion. Phys Chem Chem Phys 2012;14:1085–106.

[157] Fábri C, Mátyus E, Furtenbacher T, Mihály B, Zoltáni T, Nemes L, et al. Variational quantum mechanical and active database approaches to the rotational–vibrational spectroscopy of ketene. J Chem Phys 2011;135:094307.
[158] Furtenbacher T, Szidarovszky T, Fábri C, Császár AG. Analysis of the rotational–vibrational states of the molecular ion H_3^+. J Chem Theory Comput 2013;9:5471–8.
[159] Furtenbacher T, Szidarovszky T, Fábri C, Császár AG. Marvel analysis of the rotational–vibrational states of the molecular ions H_2D^+ and D_2H^+. Phys Chem Chem Phys 2013;15:10181–93.
[160] Bykov AD, Fazliev AZ, Filippov NN, Kozodoev AV, Privezentsev AI, Sinitsa LN, et al. Distributed information system on atmospheric spectroscopy. Geophys Res Abstr 2007;9:01906 SRef-ID:1607-7962/gra/EGU2007-A-01906.
[161] Császár AG, Fazliev AZ, Tennyson J. W@DIS—prototype information system for systematization of spectral data of water. Abstracts of the twentieth colloquium on high resolution molecular spectroscopy; 2007. URL: ⟨http://vesta.u-bourgogne.fr/hrms/⟩.
[162] Tennyson J, Bernath PF, Campargue A, Császár AG, Daumont L, Gamache RR, et al. Recommended isolated-line profile for representing high-resolution spectroscopic transitions. Pure Appl Chem, accepted for publication.